Supplementary Material

Pseudoguaianelactones A−C: Three Unusual Sesquiterpenoids with Anti-inflammatory Activities from *Lindera glauca* by Inhibiting LPS-induced Expression of iNOS and COX-2

Qingfeng Ruan,[a‡] Shiqing Jiang ,[a‡] Xiaoyun Zheng ,[a] Yuqian Tang ,[a] Bao Yang ,[a] Tao Yi ,[a] Jing Jin ,[b] Hui Cui,[*a] and Zhongxiang Zhao[*a]

[a]School of Pharmaceutical Sciences, Guangzhou University of Chinese Medicine, Guangzhou 510006, China;

[b]School of Pharmaceutical Sciences, Sun Yat-Sen University, Guangzhou 510006, China

Supporting Information Placeholder

Co-first author

* Corresponding authors: School of Pharmaceutical Sciences, Guangzhou University of Chinese Medicine, Guangzhou, 510006, China. Tel: +86 20 39358072. *E-mail address*: zzx37@gzucm.edu.cn (Z. Zhao).

* Corresponding authors: School of Pharmaceutical Sciences, Guangzhou University of Chinese Medicine, Guangzhou, 510006, China. Tel: +86 20 39358072. *E-mail address*: cuihui@gzucm.edu.cn (H. Cui).

Author Contributions

‡These authors contributed equally to this work.

Index

Experimental section

General experimental procedures

IR spectrum was obtained using a Thermo Scientific Nicolet iS 5 spectrometer (KBr pellets). Melting points were acquired on X-4 micro melting point apparatus. Optical rotations were measured on a Bellingham-Stanley ADP 440 + polarimeter at 25 ℃. UV spectra were recorded using a Shimadzu UV-2401A spectrophotometer. HRESIMS spectra were acquired on an AB Sciex Triple-TOF 5600^+ apparatus. The ^{1}H NMR (400 MHz), ^{13}C NMR (100 MHz), and 2D NMR spectra were obtained on a Bruker AVANCE-400 using TMS as an internal reference. ECD spectra were obtained on an Applied Photophysics Chirascan spectrometer. X-ray crystallographic analysis was carried out on an Agilent Gemini Ultra diffractometer with Cu Kα radiation (λ=1.54178 Å). TLC analysis was carried out on silica gel plates (Marine Chemical Ltd., Qingdao, China). High silica gel (H, Marine Chemical Ltd., Qingdao, China), Silica gel (200 - 300 mesh, Marine Chemical Ltd., Qingdao, China), RP-C18 silica gel (Fuji, 40 - 75 μm), and Sephadex LH-20 (GE Healthcare Bio-Sciences AB, Sweden) were used for column chromatography (CC). Preparative HPLC separations were carried out by photodiode array (PDA) analysis using a Kromasil 100–5 C18 column (250 × 10 mm, 5 μm) by a Wufeng LC-100 apparatus (Shanghai Wufeng Co., Ltd., China).

Plant material

The roots of *Lindera glauca* (Shan-hu-jiao in Chinese) were collected from Hubei, China, in May 2017. The roots were authenticated by Dr. Guangtian Peng of Guangzhou University of Chinese Medicine, China. A voucher specimen (ZYXY-IR-2017-05) was deposited in the School of Pharmaceutical Sciences, Guangzhou University of Chinese Medicine, China.

Extraction and Isolation

The air-dried roots (20 kg) were extracted with methanol at room temperature, and then the solvent was evaporated under reduced pressure to yield a crude extract (2.4 kg), which was suspended in distilled water (3.0 L) and partitioned with PE, $CHCl_3$, EtOAc, and n-BuOH.

The PE extract (460.0 g) was subjected to silica gel (200–300 mesh) CC, using a gradient of PE-Me_2CO (100:1–10:1, *v*/*v*), to afford eight fractions (Fr.A–Fr.H). Fr.H was separated over Sephadex LH-20 gel ($CHCl_3$-MeOH, 1:1) to give three subfractions H1-H3. Then, subfraction H1 was chromatographed via ODS CC (MeOH-H_2O, 50:50–60:40–70:30) to yield two parts H1.1 and H1.2. H1.2 was further purified by HPLC on a semipreparative RP-18 column using MeOH-H_2O system (75:25) to yield **1** (103.6 mg), **2** (9.6 mg), **3** (298.2 mg).

Spectral data

Pseudoguaianelactone A (**1**): Colorless needle crystals; mp 138 – 140 °C, $[\alpha]_D^{20}$ +47.0 (*c* 0.215, MeOH); UV (methanol) λ_{max} (log ε) 213 (3.59) nm; IR (KBr) ν_{max}: 3415, 2939, 2869, 1676, 1607, 1451, 1397, 1199, 1125, 999, 936 cm^{-1}; ^{1}H-NMR (400 MHz, $CDCl_3$) and ^{13}C-NMR (100 MHz, $CDCl_3$) data, see Table S1; (–) HRESIMS *m/z* 249.1496 $[M - H]^-$ (calcd for $C_{15}H_{21}O_3$ 249.1491).

Pseudoguaianelactone B (**2**): Colorless oil; $[\alpha]_D^{20}$ -157.3 (*c* 0.206, MeOH); UV (methanol) λ_{max} (log ε) 204 (4.18) nm; IR (KBr) ν_{max}: 3480, 2955, 2922, 2872, 1697, 1628, 1451, 1371, 1149, 1093, 1003, 938 cm^{-1}; ^{1}H-NMR (400 MHz, $CDCl_3$) and ^{13}C-NMR (100 MHz, $CDCl_3$) data, see Table S1; ECD (*c* 1.11 mM, MeOH) λ_{max} ($\Delta\varepsilon$) 204 (-22.70) and 251 (5.30) nm; (–) HRESIMS data at *m*/*z* 249.1499 $[M-H]^-$ (calcd for $C_{15}H_{21}O_3$, 249.1491).

Pseudoguaianelactone C (**3**): Colorless needle crystals; mp 145–146 ℃; $[\alpha]_D^{20}$ -65.2 (*c* 0.204, MeOH); UV (methanol) λ_{max} (log ε) 213 (4.09) nm; IR (KBr) ν_{max}: 3417, 2929, 1746, 1603, 1573, 1470, 1418, 1384, 1215, 1081, 1020 cm^{-1}; ^{1}H-NMR (400 MHz, $CDCl_3$) and ^{13}C-NMR (100 MHz, $CDCl_3$) data, see Table S1; (–) HRESIMS ($[M-H]^-$, *m*/*z* 249.1498, calcd for 249.1491).

Table S1 ^{1}H (400 MHz) and ^{13}C (100 MHz) NMR data for compounds **1**–**3** in $CDCl_3$ (δ in ppm and *J* in Hz)**.**

Position	**1**		**2**		**3**	
	δ_C	δ_H	δ_C	δ_H	δ_C	δ_H
1	100.5		56.4	2.22 td (9.2, 5.2)	49.3	2.53 td (9.2, 5.2)
2	37.1	2.01 m	22.4	1.68 m	23.5	1.71 m, 1.86 m
3	32.6	1.50 m, 1.73 m	38.3	1.92 m	37.9	1.68 m, 2.10 m
4	36.7	2.19 m	82.9		83.9	
5	40.0	3.00 m	93.7		96.8	
6	28.1	1.56 m, 1.86 m	40.3	1.99 overlap, 2.51 d (14.4)	30.0	1.97 m, 2.06 m
7	36.9	3.00 overlap	40.6	2.80 brs	35.3	3.03 brs
8	26.1	1.68 m, 1.96 m	34.6	1.72 m	31.3	1.95 m
9	37.2	1.67 m	28.0	1.71 m	30.7	1.50 m, 1.75 m
10	73.8		35.1	2.03 m	31.6	2.13 m
11	144.0		147.9		140.4	
12	168.5		172.7		165.7	
13	128.7	5.45 s, 6.34 s	123.1	5.36 s, 5.69 s	125.6	5.44 s, 6.27 s
14	26.9	1.30 s	21.6	0.87 d (6.8)	16.5	0.94 d (7.2)
15	16.5	0.94 d (6.8)	18.3	1.44 s	21.5	1.19 s

X-ray crystallographic analysis of compounds 1 and 3.

The single-crystal X-ray diffraction data were collected at 100K for **1** and **3** on an Agilent Gemini Ultra diffractometer with Cu Kα radiation (λ = 1.541 78 Å). The structures were solved by direct methods (SHELXS-97) and refined using full-matrix least-squares difference Fourier techniques. Hydrogen atoms bonded to carbons were placed on the geometrically ideal positions by the "ride on" method. Hydrogen atoms bonded to oxygen were located by the difference Fourier method and were included in the calculation of structure factors with isotropic temperature factors. Crystallographic data for **1** and **3** have been deposited with the Cambridge Crystallographic Data Centre. Copies of the data can be obtained, free of charge, on application to the Director, CCDC（1945205 and 1945206）, 12 Union Road, Cambridge CB2 1EZ, UK (fax: 44-(0)1223-336033, or e-mail: deposit@ccdc.cam.ac.uk).

Crystal data of **1**: $C_{15}H_{22}O_3$, (M = 250.32 g/mol), monoclinic, space group, P_{21}, a = 16.79540 (10) Å, b = 10.61320(10) Å, c = 16.87830(10) Å; α=90 °, β = 119.0570 °(10), γ = 90 °, V = 2629.93 (4) $Å^3$, Z = 8, T =

100.00 (10) K, μ (Cu Kα) = 0.692 mm^{-1}, *Dcalc* = 1.264 g/cm^3, F(000) = 1088.0, crystal size: 0.3 × 0.2 × 0.1 mm^3. Independent reflections: 10381 (R_{int} = 0.0520). The final R1 values were 0.0309, wR2 = 0.0791 [$I > 2\sigma(I)$]. The goodness of fit on F^2 was 1.049. Flack parameter = -0.07 (5).

Crystal data of **3**: $C_{15}H_{22}O_3$, (M = 250.32 g/mol), tetragonal, space group, P_{41212}, a = 9.72709 (4) Å, b = 9.72709 (4), c = 28.60837 (18) Å; $\alpha = \beta = \gamma = 90°$, V = 2706.82 (3) $Å^3$, Z = 8, T = 100.01 (10) K, μ (Cu Kα) = 0.672 mm^{-1}, *Dcalc* = 1.229 g/cm^3, F(000) = 1088.0, crystal size: 0.3 × 0.2 × 0.1 mm^3. Independent reflections: 2656 (R_{int} = 0.0375). The final R1 values were 0.0261, wR2=0.0686 [$I > 2\sigma(I)$]. The goodness of fit on F^2 was 1.072. Flack parameter = 0.00 (5).

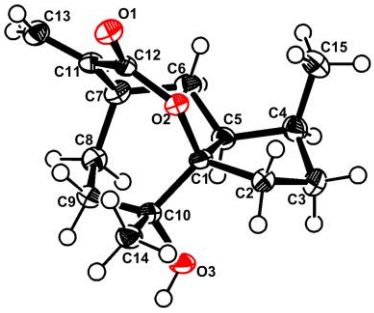

1

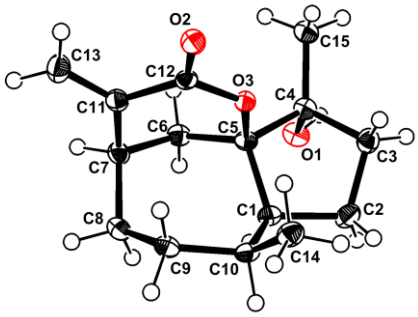

3

Table S2 Crystal data and structure refinement for compounds **1** and **3**

Item	Compound **1**	Compound **3**
CCDC number	1945205	1945206
Emprical formula	$C_{15}H_{22}O_3$	$C_{15}H_{22}O_3$
Formula weight	250.32	250.32
Temperature/K	100.00(10)	100.01(10)
Crystal color and form	Colourless block	Colourless block
Radiation type	CuK\α (λ = 1.54184)	CuK\α (λ = 1.54184)
Crystal system	monoclinic	tetragonal
Space group	$P2_1$	$P4_12_12$
a/Å	16.79540(10)	9.72709(4)
b/Å	10.61320(10)	9.72709(4)
c/Å	16.87830(10)	28.60837(18)
α/°	90	90
β/°	119.0570(10)	90
γ/°	90	90
Volume $Å^3$	2629.93(4)	2706.82(3)
Z	8	8
Density (calculated)	1.264	1.229
F(000)	1088.0	1088.0
Crystal size/mm^3	0.3 × 0.2 × 0.1	0.3 × 0.2 × 0.1
μ /mm^{-1}	0.692	0.672
θ range/ °	5.99 to 144.242	9.604 to 144.142
Index ranges	-20 ≤ h ≤ 20, -13 ≤ k ≤ 13, -20 ≤ l ≤ 20	-12 ≤ h ≤ 11, -12 ≤ k ≤ 12, -34 ≤ l ≤ 35
Reflections collected/unique	53491	28910
Independent reflections	10381 [R_{int} = 0.0520, R_{sigma} = 0.0340]	2656 [R_{int} = 0.0375, R_{sigma} = 0.0154]
Data/restraints/parameters	10381/1/693	2656/0/174

Goodness-of-fit on F^2	1.049	1.072
Fianl R indexes [I > 2σ(I)]	R_1 = 0.0309, wR_2 = 0.0791	R_1 = 0.0261, wR_2 = 0.0686
Fianl R indexes (all data)	R_1 = 0.0319, wR_2 = 0.0800	R_1 = 0.0266, wR_2 = 0.0690
Largest diff. peak/hole / e Å^{-3}	0.19/-0.18	0.18/-0.15
Flack parameter	-0.07(5)	0.00(5)

ECD calculation details

1. Methods

Monte Carlo conformational searches were carried out by means of the Spartan's 10 software using Merck Molecular Force Field (MMFF). Only two conformers were obtained and chosen for optimization at B3LYP/6-31g (d, p) level in gas. The theoretical calculation of ECD was conducted in MeOH using Time-dependent Density functional theory (TD-DFT) at the B3LYP/6-311+g (d, p) level for all conformers of compound **2**. Rotatory strengths for a total of 30 excited states were calculated. ECD spectra were generated using the program SpecDis 1.6 (University of Würzburg, Würzburg, Germany) and GraphPad Prism 5 (University of California San Diego, USA) from dipole-length rotational strengths by applying Gaussian band shapes with sigma = 0.3 eV.

2. Results

Table S3 Gibbs free energies[a] and equilibrium populations[b] of low-energy conformers of 5*S*-**2.**

Conformers of 5*S*-**2**	In MeOH	
	Δ*G*	*P* (%)/100
2a	0.00	1.000
2b	5.56	0.000

[a]B3LYP/6-31G(d,p), in kcal/mol. [b]From Δ*G* values at 298.15K.

Table S4 Cartesian coordinates for the low-energy reoptimized MMFF conformers of **2** at B3LYP/6-311+G(d,p) level of theory in CH_3OH**.**

Conformer **2a**		Standard Orientation (Ångstroms)			
Center number	Atomic number	Atomic Type	X	Y	Z
1.	6.	0.	0.184889	2.202447	1.588426
2.	6.	0.	0.032881	1.927807	0.066359
3.	6.	0.	0.628028	0.559391	-0.026663
4.	6.	0.	-0.517952	-0.338613	-0.391452
5.	6.	0.	-1.021477	-1.174940	0.770672
6.	6.	0.	-0.507330	-0.615733	2.165457
7.	6.	0.	-0.627490	1.010406	2.323180
8.	6.	0.	-0.037469	-1.121509	-1.586235
9.	6.	0.	-1.008806	-2.337380	-1.446524
10.	6.	0.	-0.895744	-2.605498	0.124602
11.	6.	0.	1.388452	-1.669249	-1.698839
12.	6.	0.	0.402783	2.433191	-1.328671
13.	6.	0.	0.256549	1.388404	-2.580640
14.	8.	0.	0.415500	1.845609	-3.678550
15.	6.	0.	0.856807	3.636231	-1.684625
16.	6.	0.	0.793616	-1.230052	2.713272

17.	1.	0.	-2.095197	-0.981699	0.805412
18.	8.	0.	-0.113405	-0.042408	-2.661196
19.	8.	0.	-1.761997	0.286783	-0.833604
20.	1.	0.	1.232247	2.220489	1.912530
21.	1.	0.	-0.282737	3.133291	1.931826
22.	1.	0.	-1.050191	1.840940	-0.021370
23.	1.	0.	1.427099	0.540891	-0.762636
24.	1.	0.	1.112118	0.237894	0.882725
25.	1.	0.	-1.274758	-0.927216	2.886536
26.	1.	0.	-0.482051	1.178495	3.397328
27.	1.	0.	-1.685477	1.226512	2.130495
28.	1.	0.	-0.720382	-3.212631	-2.034831
29.	1.	0.	-2.036580	-2.066278	-1.694581
30.	1.	0.	0.063317	-3.084901	0.347706
31.	1.	0.	-1.679439	-3.292922	0.456287
32.	1.	0.	1.624297	-2.376065	-0.899115
33.	1.	0.	1.459013	-2.204193	-2.650515
34.	1.	0.	2.154487	-0.893993	-1.709288
35.	1.	0.	0.999730	4.401704	-0.928019
36.	1.	0.	1.093162	3.878809	-2.713147
37.	1.	0.	1.024660	-0.819786	3.702629
38.	1.	0.	1.675205	-1.074841	2.084187
39.	1.	0.	0.673590	-2.312996	2.828305
40.	1.	0.	-1.698949	0.436609	-1.788431

Conformer **2b**		Standard Orientation (Ångstroms)			
Center number	Atom number	Type	X	Y	Z
1.	6.	0.	0.118720	2.194073	1.609792
2.	6.	0.	0.094799	1.935622	0.077633
3.	6.	0.	0.679914	0.560982	0.019113
4.	6.	0.	-0.426325	-0.305688	-0.498932
5.	6.	0.	-1.103255	-1.129706	0.584706
6.	6.	0.	-0.734975	-0.609622	2.042977
7.	6.	0.	-0.798921	1.017481	2.239176
8.	6.	0.	0.184775	-1.102988	-1.620449
9.	6.	0.	-0.837881	-2.285160	-1.621244
10.	6.	0.	-0.953706	-2.563287	-0.055349
11.	6.	0.	1.590492	-1.709811	-1.500440
12.	6.	0.	0.560670	2.411345	-1.306665
13.	6.	0.	0.361880	1.379332	-2.572456
14.	8.	0.	0.337508	1.908353	-3.651994
15.	6.	0.	1.117436	3.577462	-1.633204
16.	6.	0.	0.469892	-1.293246	2.713690
17.	1.	0.	-2.179821	-0.930775	0.517629
18.	8.	0.	0.324679	-0.062432	-2.680251
19.	8.	0.	-1.514256	0.373095	-1.210838
20.	1.	0.	1.130038	2.169336	2.031177
21.	1.	0.	-0.348348	3.134817	1.925825
22.	1.	0.	-0.978720	1.889586	-0.090292
23.	1.	0.	1.548496	0.556871	-0.632300
24.	1.	0.	1.056500	0.206461	0.966815
25.	1.	0.	-1.590937	-0.904064	2.664840
26.	1.	0.	-0.743551	1.146446	3.326902
27.	1.	0.	-1.829709	1.289512	1.971753
28.	1.	0.	-0.502045	-3.172148	-2.165365
29.	1.	0.	-1.804085	-1.969662	-2.018389
30.	1.	0.	-0.055293	-3.078617	0.297600

31.	1.	0.	-1.802889	-3.215048	0.169531
32.	1.	0.	1.667946	-2.450079	-0.700092
33.	1.	0.	1.800183	-2.217053	-2.446906
34.	1.	0.	2.372473	-0.964068	-1.358037
35.	1.	0.	1.285158	4.333005	-0.871400
36.	1.	0.	1.407320	3.803022	-2.652137
37.	1.	0.	0.610383	-0.909357	3.729980
38.	1.	0.	1.418410	-1.168261	2.183839
39.	1.	0.	0.289238	-2.370631	2.792667
40.	1.	0.	-2.224193	0.524904	-0.576906

Anti-inflammatory Assay and Cell Viability

RAW264.7 macrophages were kindly gifted from Professor Lian Zhou from the School of Pharmaceutical Sciences, Guangzhou University of Chinese Medicine. As our previously reported with slight modifications, [1-2] RAW264.7 cells were cultured in DMEM supplemented with 10% FBS with penicillin G (60 units/mL) and streptomycin (100 μg/mL) in a humidified 5% CO_2 air atmosphere at 37 ℃. The cells were harvested with trypsin-EDTA and diluted and suspended in fresh medium. The tested samples were dissolved in DMSO and diluted with DMEM medium until the final concentration < 0.1%. The suspended cells were seeded in 96-well plates (2×10^4 cells/well) and allowed to adhere for 24 h. To determine the inhibitory activity of each compound, the cells were pretreated with fresh medium (200 μL/well) containing the tested compounds at various final concentrations (0−100 μM) for 2 h, then the LPS (1 μg/mL, Sigma, St. Louis, MO) was added and cultured for another 48 h. For the positive control group, the cells were coincubated with indomethacin. The NO concentration was detected by the Griess reagent.[3] Briefly, 100 μL of cell-free supernatant was mixed with an equal volume of Griess reagent (0.2% naphthylenediamide dihydrochloride and 2% sulfanilamide in 5% H_3PO_4) and agitated at room temperature. The optical density was measured at 540 nm using a microplate reader (Bio-Rad Laboratories, Inc., Kyoto, Japan). Sodium nitrite was used to prepare a standard curve in the assay. The experiments were performed in parallel three times. Cell viability was evaluated using an MTT assay. All the compounds were prepared as stock solutions in DMSO (final solvent concentration < 0.1% in all assays).

1 Q. F. Ruan, X. H. Zhou, S. Q. Jiang, B. Yang, J. Jin, H. Cui and Z. X. Zhao, *Fitoterapia* 2019, **134**, 50.

2 Y. Liu, Q. Ruan, S. Jiang, Y. Qu, J. Chen, M. Zhao, B. Yang, Y. Liu, Z. Zhao and H. Cui, *Fitoterapia* 2019, **137**, 104187.

3 H. Ghouila, A. Beyaoui, H. B. Jannet, B. Hamdi, A. B. Salah and Z. Mighri, *Cheminform* 2010, **40**, 1563.

Western Blotting

RAW264.7 cells were seeded in 6-well plates, incubated with or without compounds **1**–**3** for 18 h, then fixed with or without LPS (1 μg/mL) for 6 h. The cell lysates were prepared with RIPA lysis buffer (50 mM Tris-Cl, pH 7.4, 150 mM NaCl, 0.1% SDS, 1% NP-40, 1% sodium deoxycholate, 1 mM phenylmethyl-sulfonylfluoride, 1 μg/ml pepstatin, 1 μg/ml leupeptin, and 1 μg/ml aprotinin) fixed with a protease inhibitor cocktail and a phosphatase inhibitor. The concentrations of protein were determined by Pierce Rapid Gold BCA Protein Assay Kit (Beyotime, China). Equal amounts (20 μg) of protein of each sample was electrophoresed in 8% SDS-PAGE, and then transferred to 0.45 μm polyvinylidene difluoride

(PVDF: Millipore, Bedford, MA) western membrane. The membranes were soaked in blocking buffer (5% skimmed milk in TBST) for 2 h. Then the membranes were incubated with primary antibodies at 4 ℃ overnight. After being washed by TBST three times, the membranes were incubated with corresponding secondary antibody at room temperature for 2 h. Following three washes in TBST, immunoreactive bands were visualized by the enhanced chemiluminescence (ECL) (Millipore, Billerica, MA). Finally, immunoreactive signals were detected using Chemiluminescence imager (Tanon 5200CE, Shanghai, China).

Table S5 Primary antibodies used in this study.

Primary antibodies	Dilution	Source
β-actin Mouse Antibody	1:1000	Boster
iNOS Rabbit Antibody	1:1000	Abcam
COX-2 Rabbit Antibody	1:1000	CST
Mouse secondary Antibody	1:1000	Boster
Rabbit secondary Antibody	1:1000	Boster

Enzyme-linked immunosorbent assay (ELISA)

RAW264.7 cells were plated into 96-well plates (5×10^4 cells/well). Cells were pretreated with **1**–**3** for 2 h and then stimulated with 1 μg/ml LPS for 24 h. The levels of TNF-α, IL-6, IL-1β and PGE_2 in the culture medium were measured by ELISA kits (Mlbio, China) according to the manufacturer's instructions.

Data analysis

Results were expressed as mean ± SD and analyzed using one-way analysis of variance (ANOVA) followed by Dunnett's tests for multiple comparisons or unpaired Student's t-tests for two-group comparisons. All analyses were performed using Prism 6.0 (GraphPad Software, San Diego, CA, USA). Statistical significance was accepted for *P*-values < 0.05.

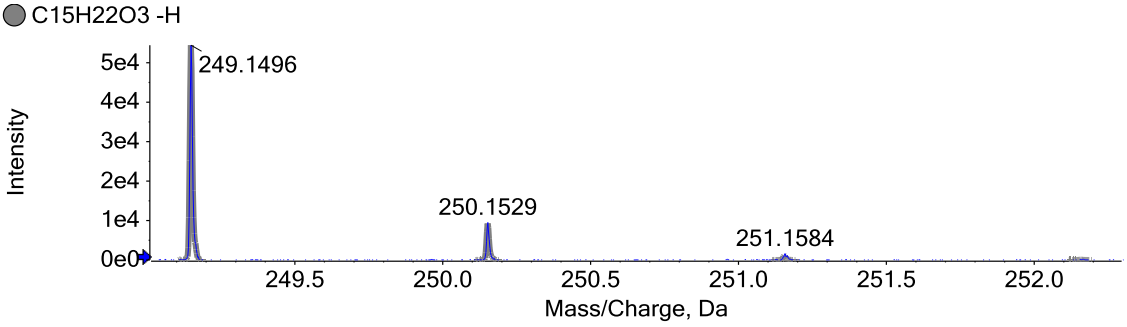

Figure S1 HR-ESI-TOF-MS spectrum of compound **1**

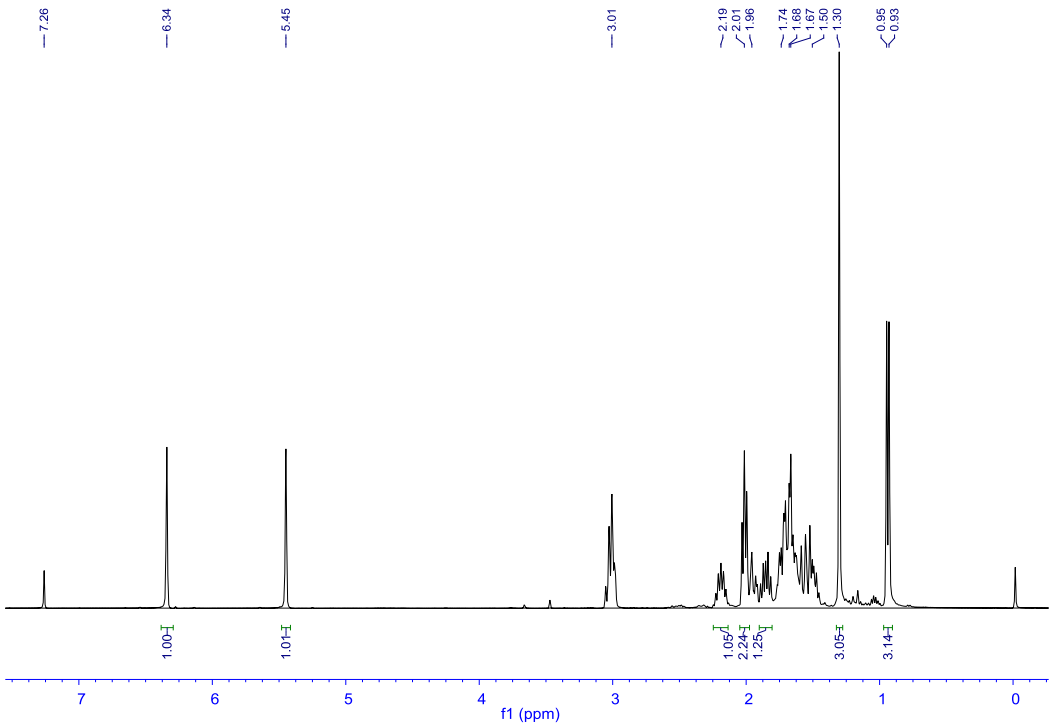

Figure S2 ^{1}H-NMR spectrum of compound **1** (400 MHz, $CDCl_3$)

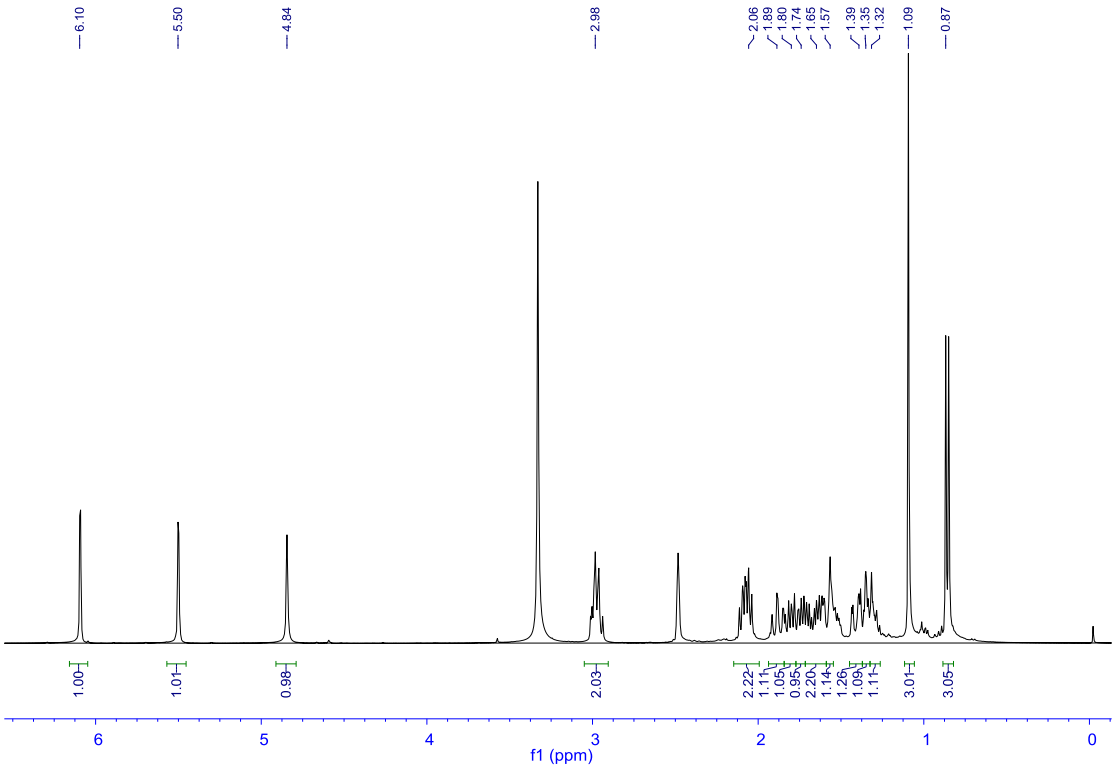

Figure S3 ^{1}H-NMR spectrum of compound **1** (400 MHz, DMSO-d_6)

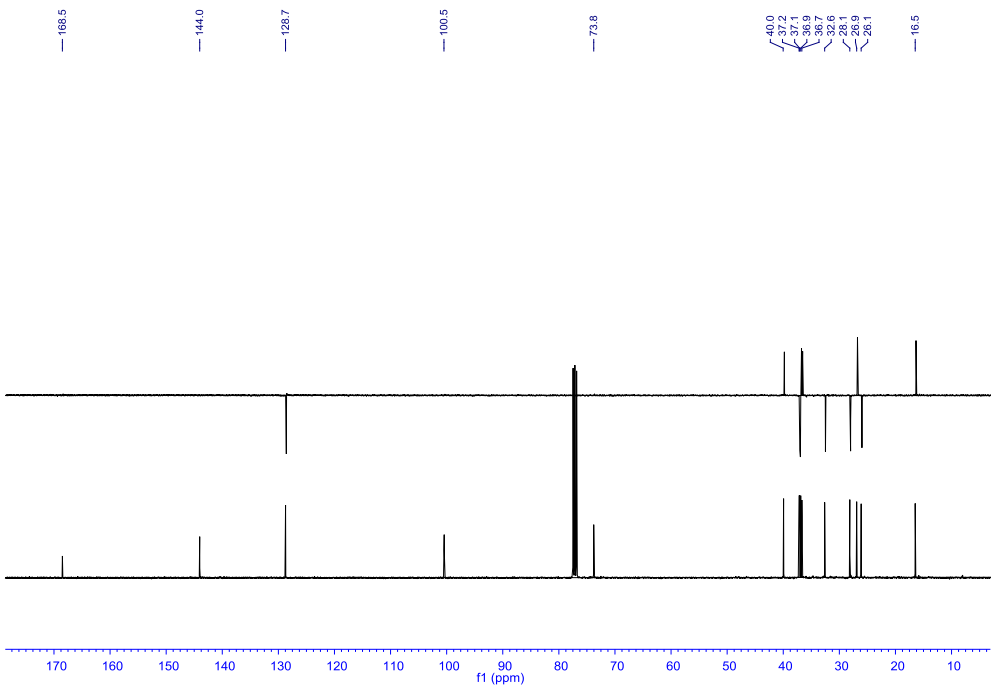

Figure S4 ^{13}C-NMR spectrum of compound **1** (100 MHz, $CDCl_3$)

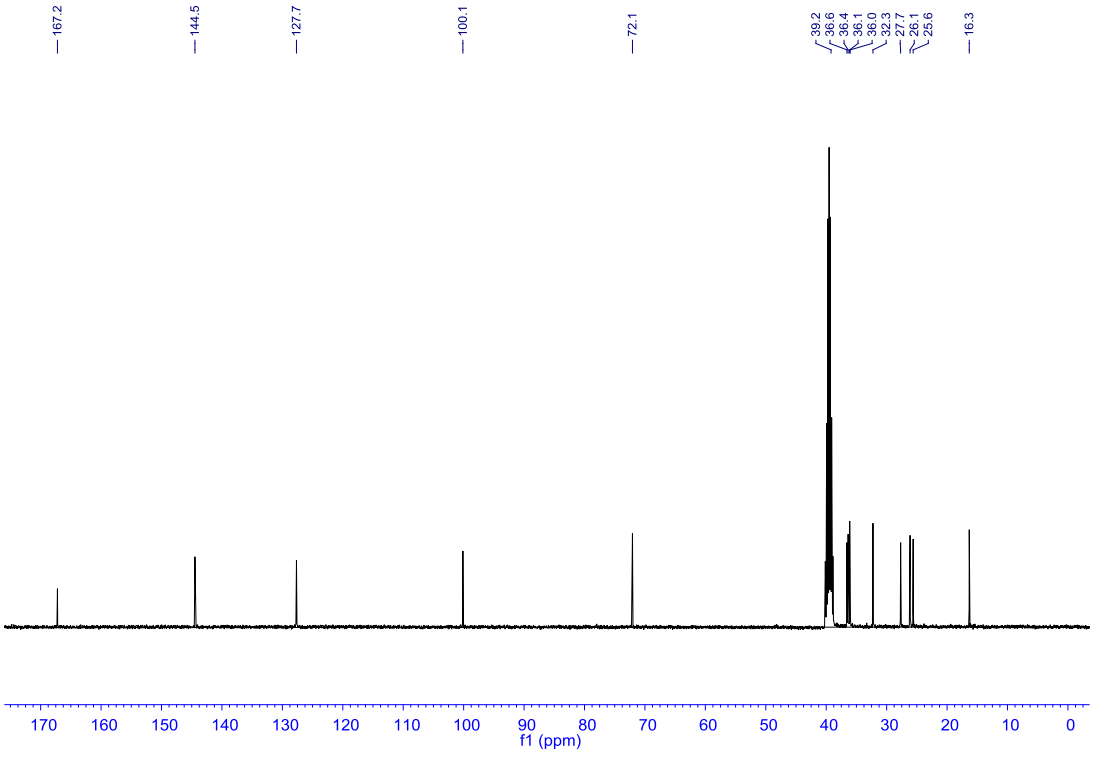

Figure S5 ^{13}C-NMR spectrum of compound **1** (100 MHz, DMSO-d_6)

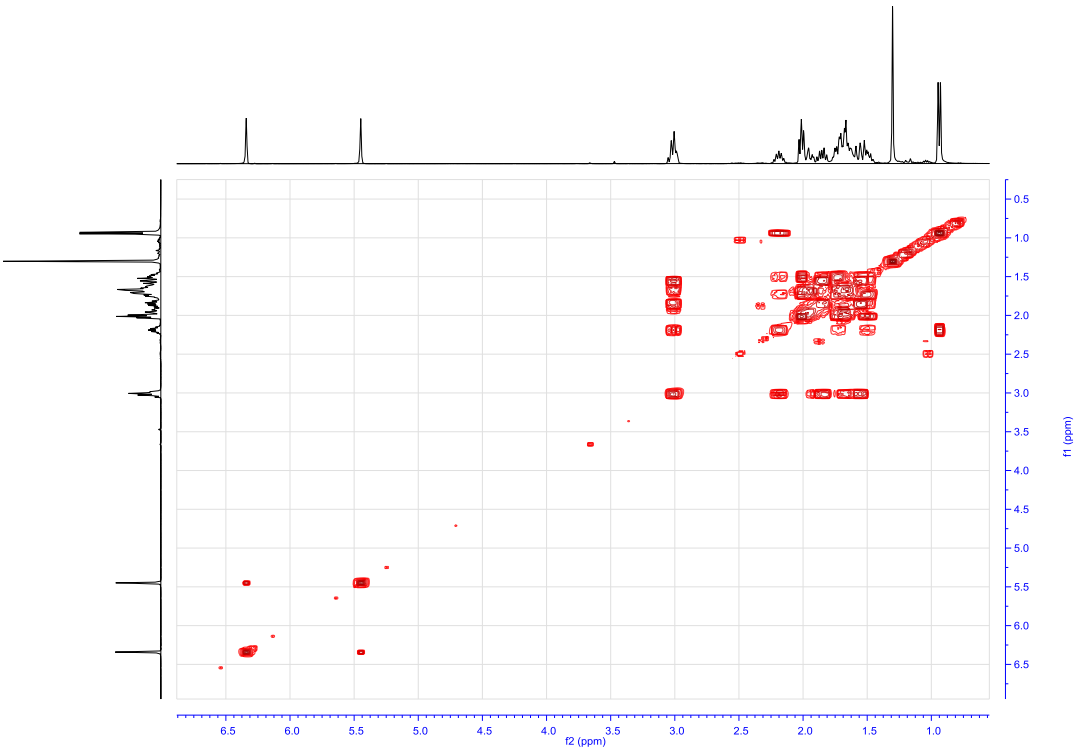

Figure S6 ^{1}H-^{1}H COSY spectrum of compound **1** (400 MHz, $CDCl_3$)

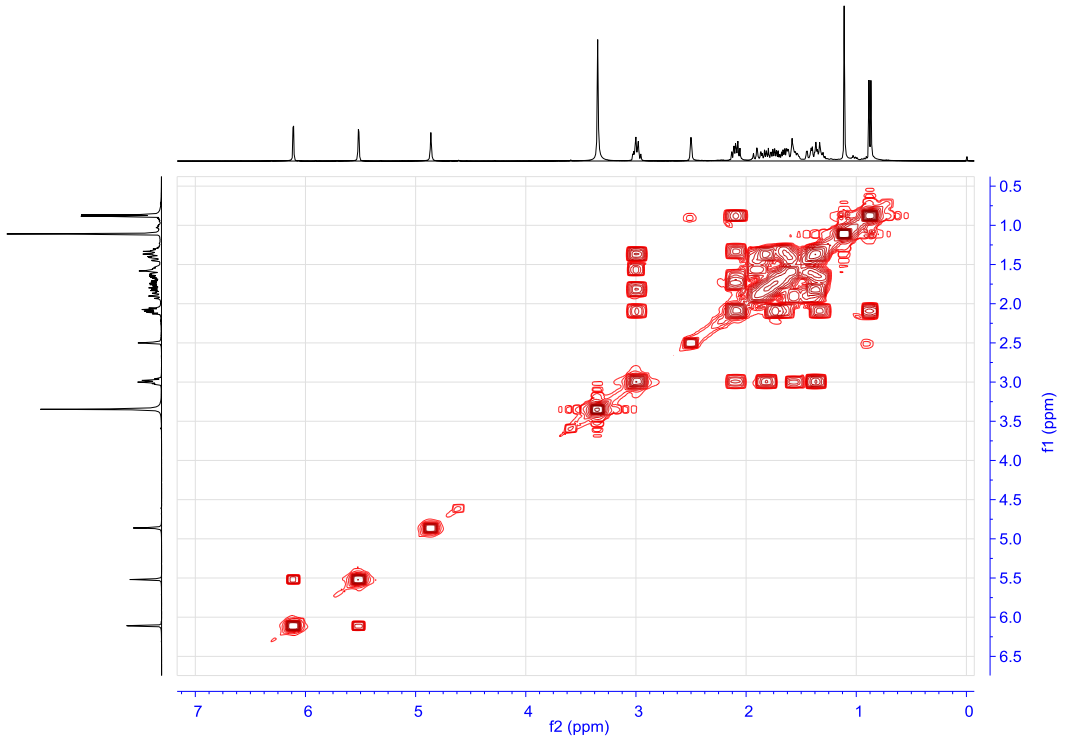

Figure S7 ^{1}H-^{1}H COSY spectrum of compound **1** (400 MHz, DMSO-d_6)

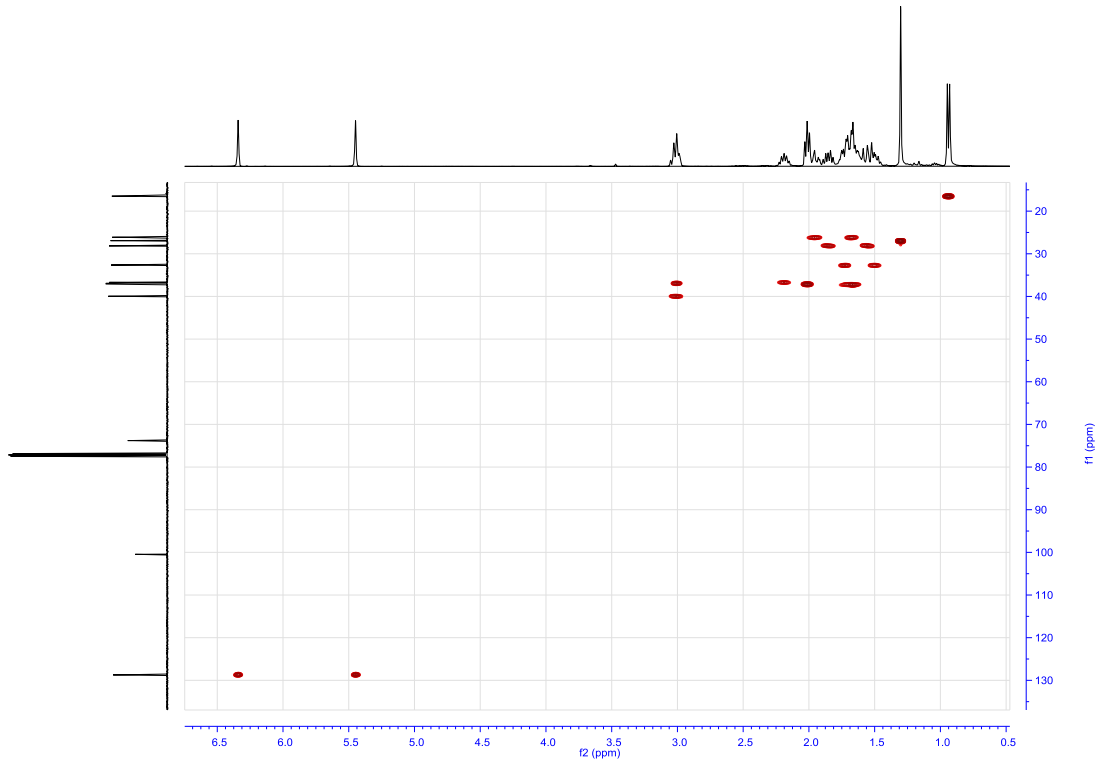

Figure S8 HSQC spectrum of compound **1** (400 MHz, $CDCl_3$)

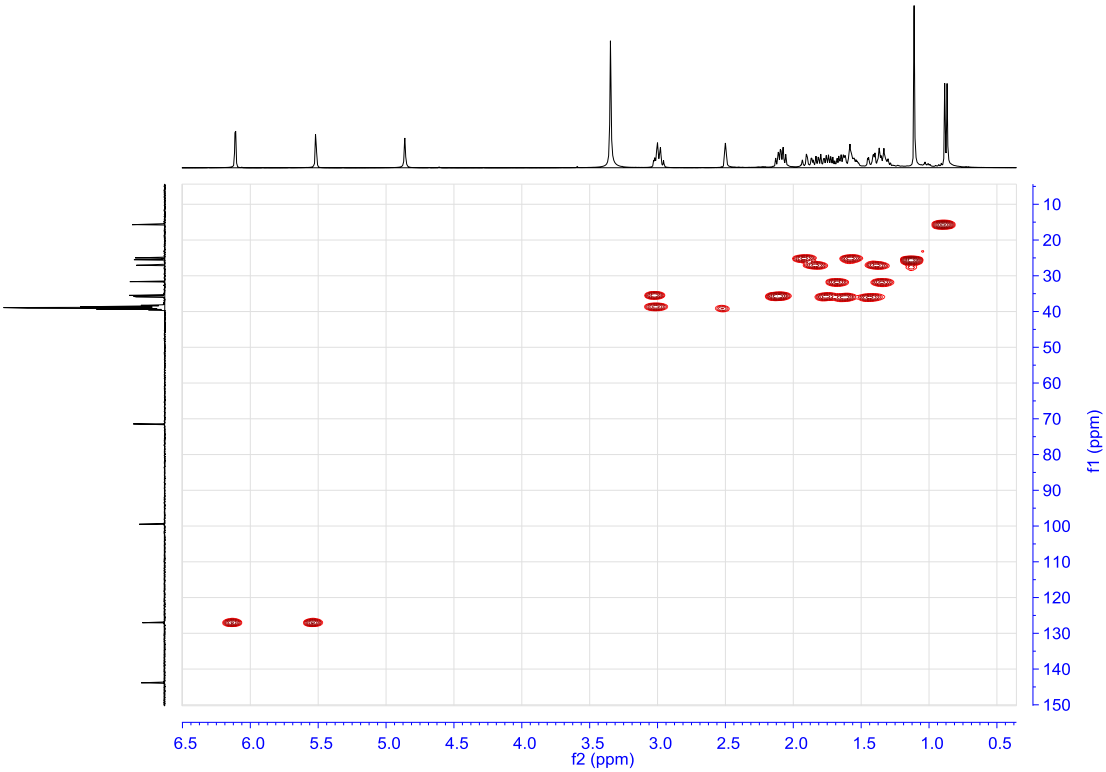

Figure S9 HSQC spectrum of compound **1** (400 MHz, DMSO-d_6)

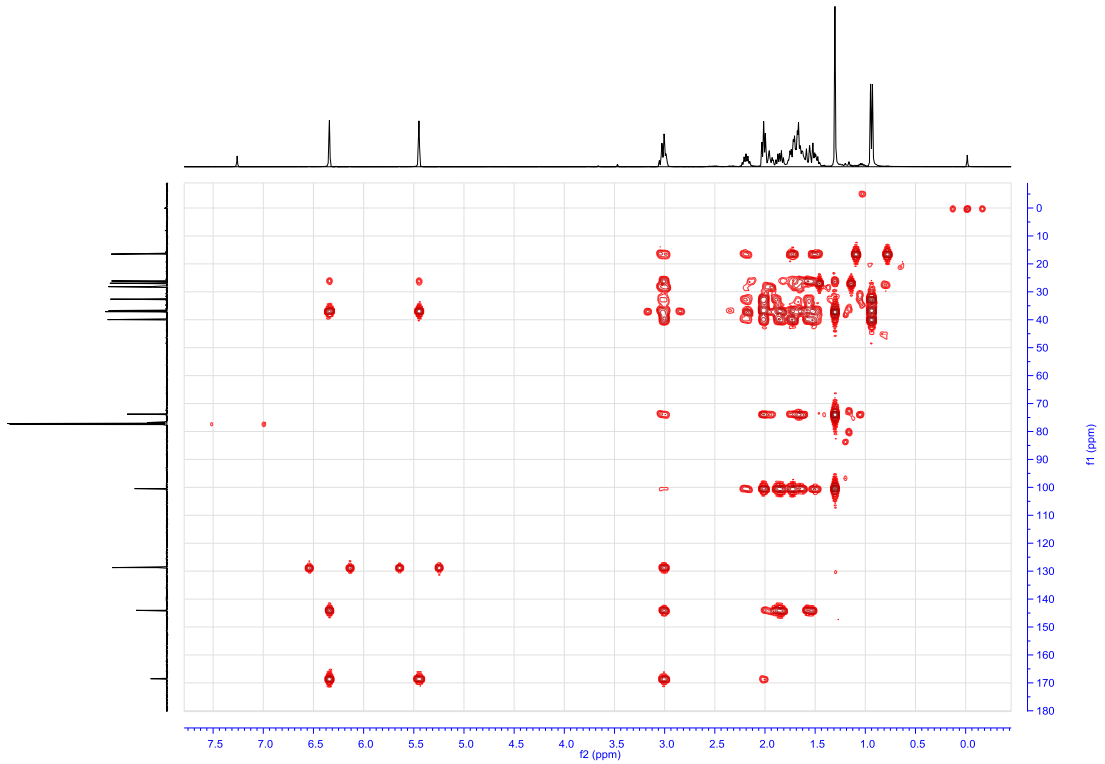

Figure S10 HMBC spectrum of compound **1** (400 MHz, $CDCl_3$)

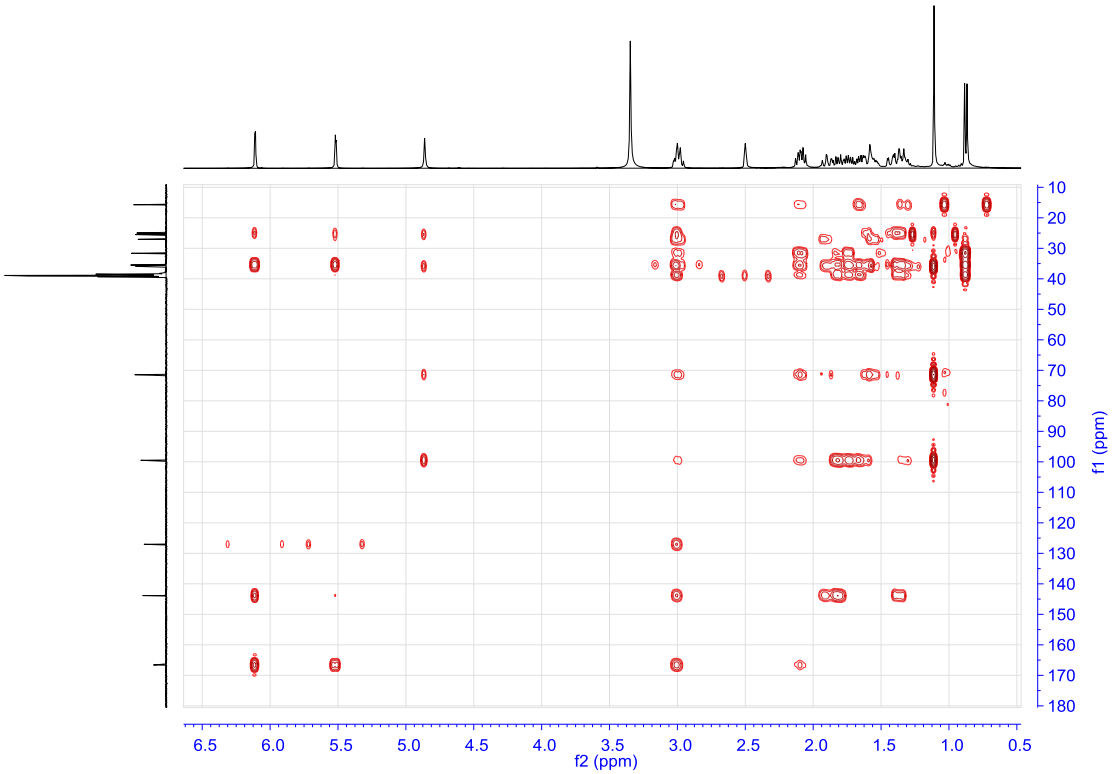

Figure S11 HMBC spectrum of compound **1** (400 MHz, DMSO-d_6)

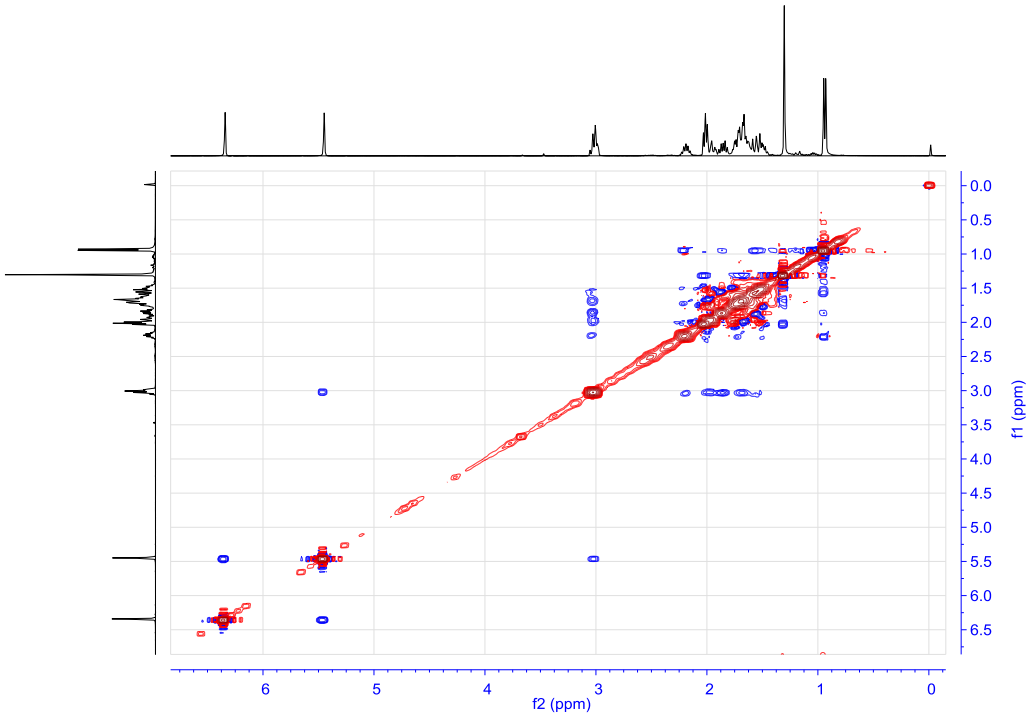

Figure S12 NOESY spectrum of compound **1** (400 MHz, $CDCl_3$)

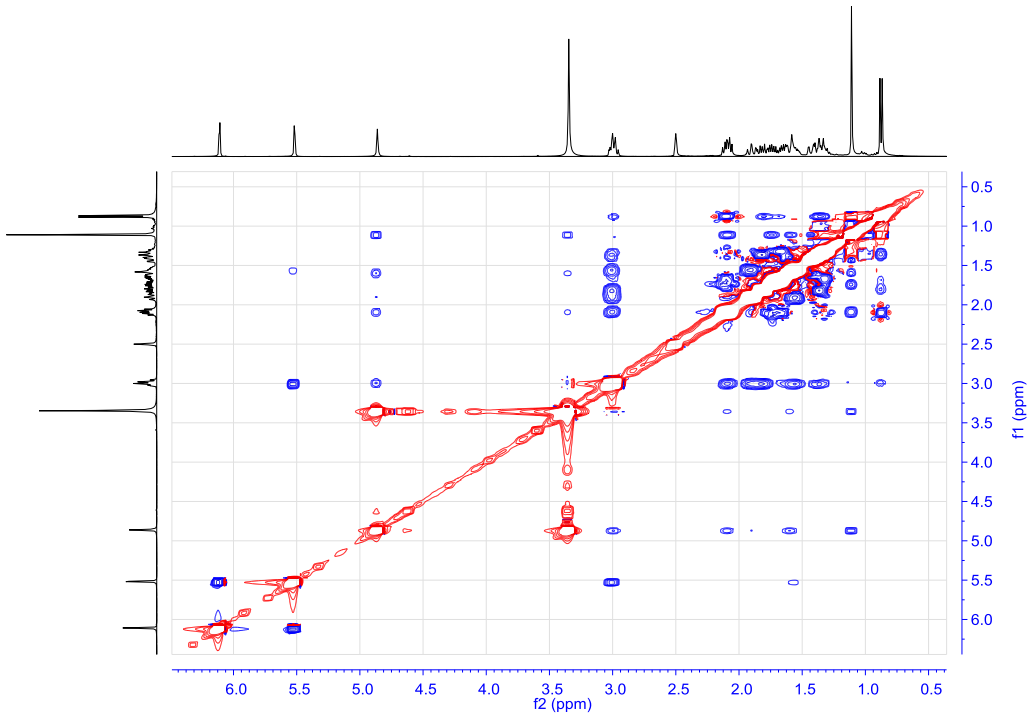

Figure S13 NOESY spectrum of compound **1** (400 MHz, DMSO-d_6)

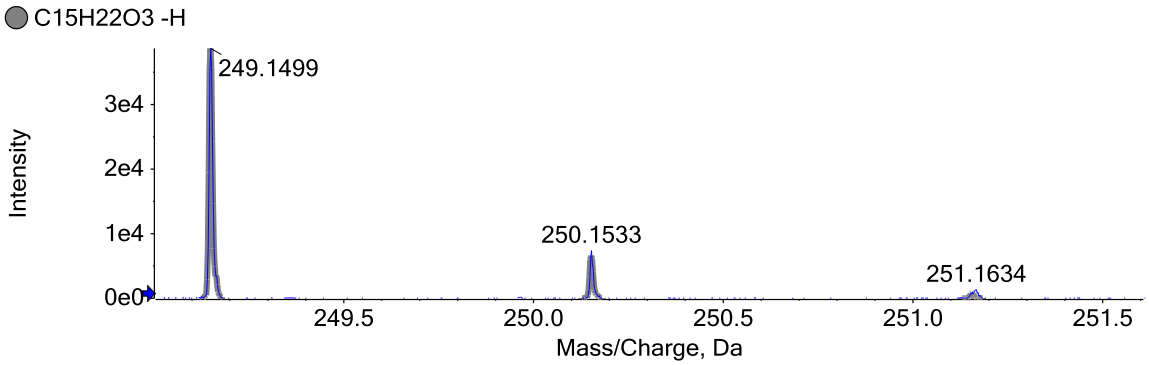

Figure S14 HR-ESI-TOF-MS spectrum of compound **2**

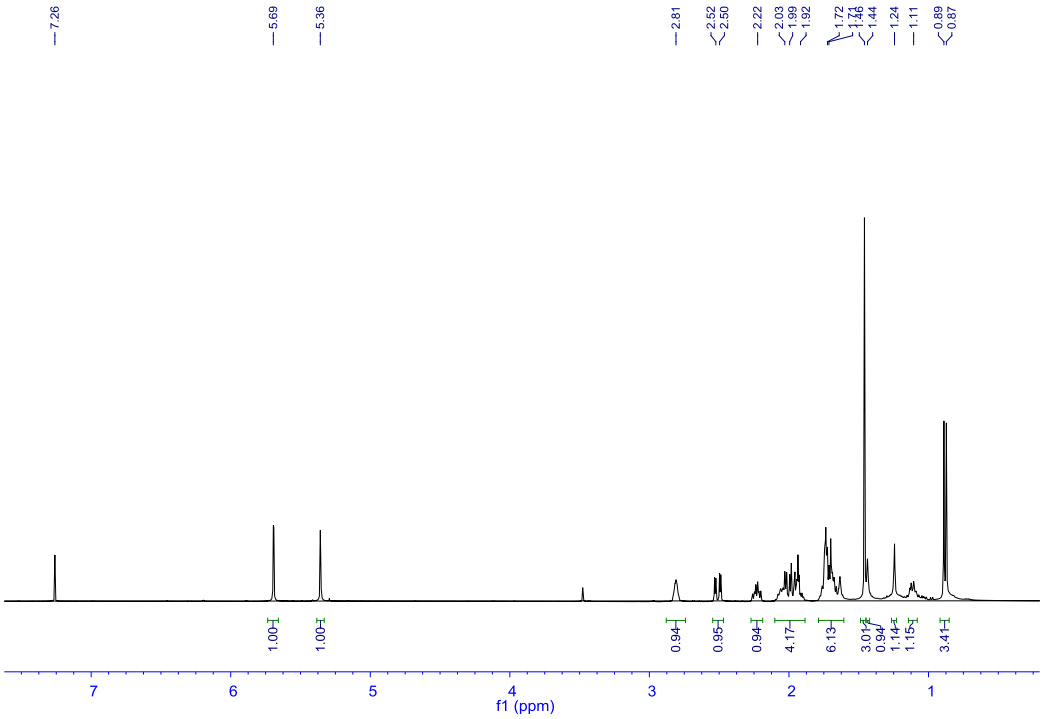

Figure S15 ^{1}H-NMR spectrum of compound **2** (400 MHz, $CDCl_3$)

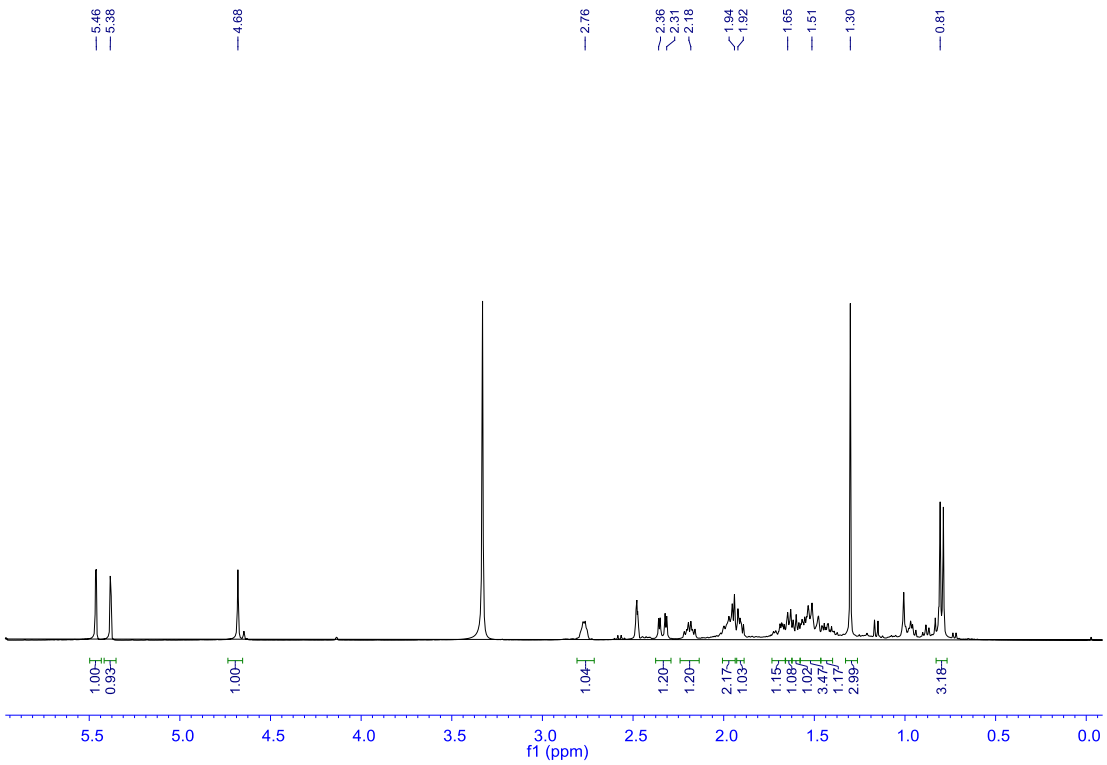

Figure S16 ^{1}H-NMR spectrum of compound **2** (400 MHz, DMSO-d_6)

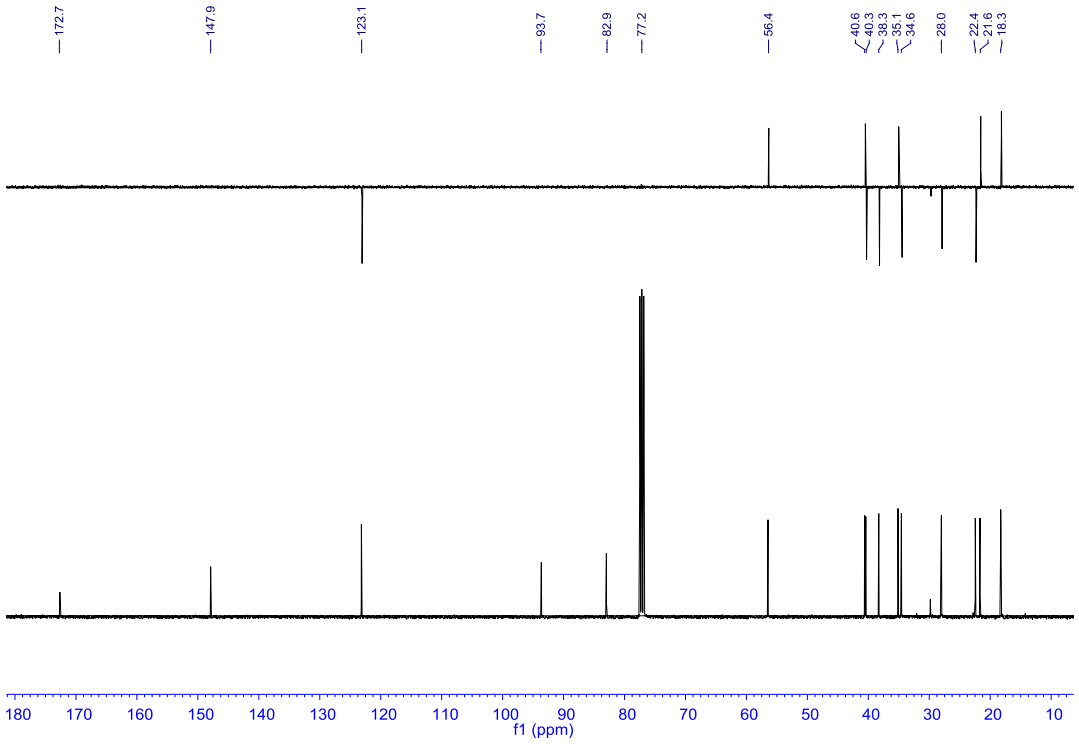

Figure S17 ^{13}C-NMR spectrum of compound **2** (100 MHz, $CDCl_3$)

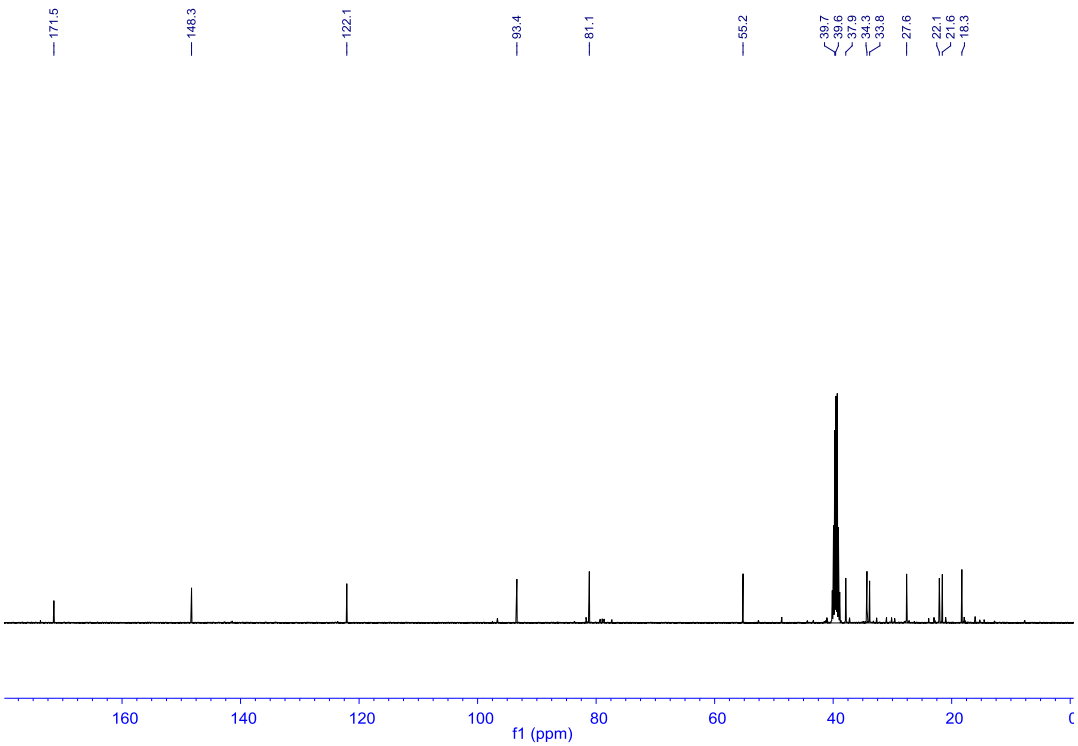

Figure S18 ^{13}C-NMR spectrum of compound **2** (100 MHz, DMSO-d_6)

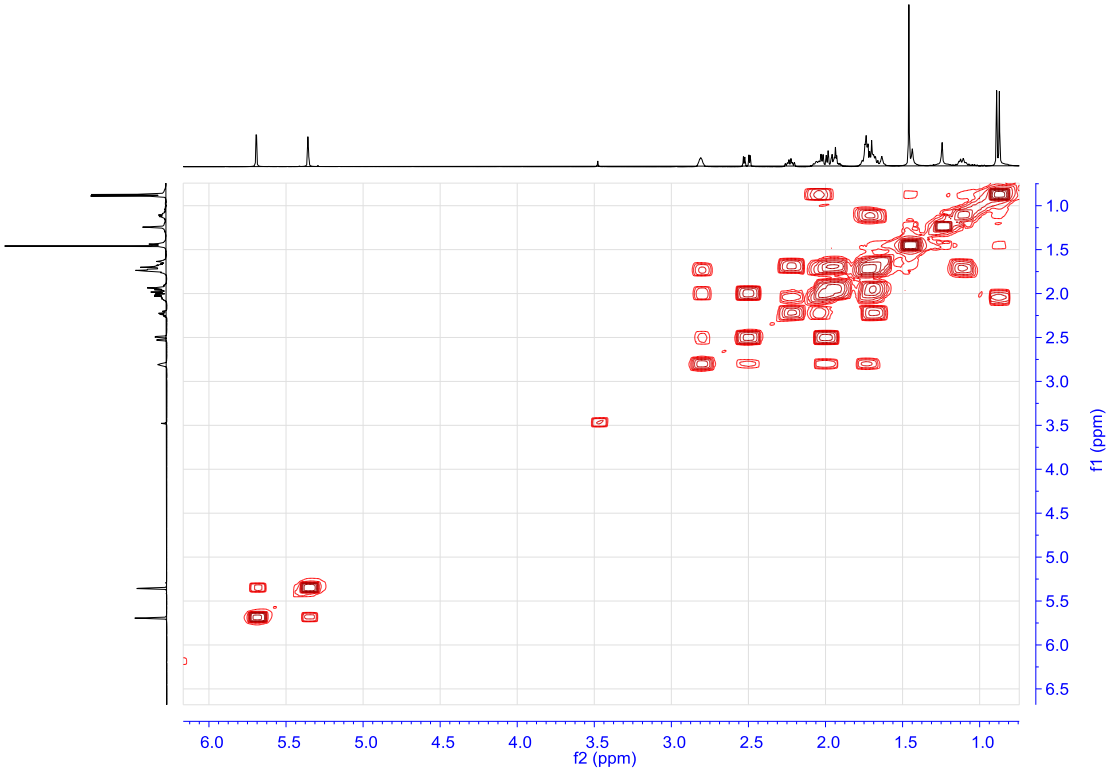

Figure S19 ^{1}H-^{1}H COSY spectrum of compound **2** (400 MHz, $CDCl_3$)

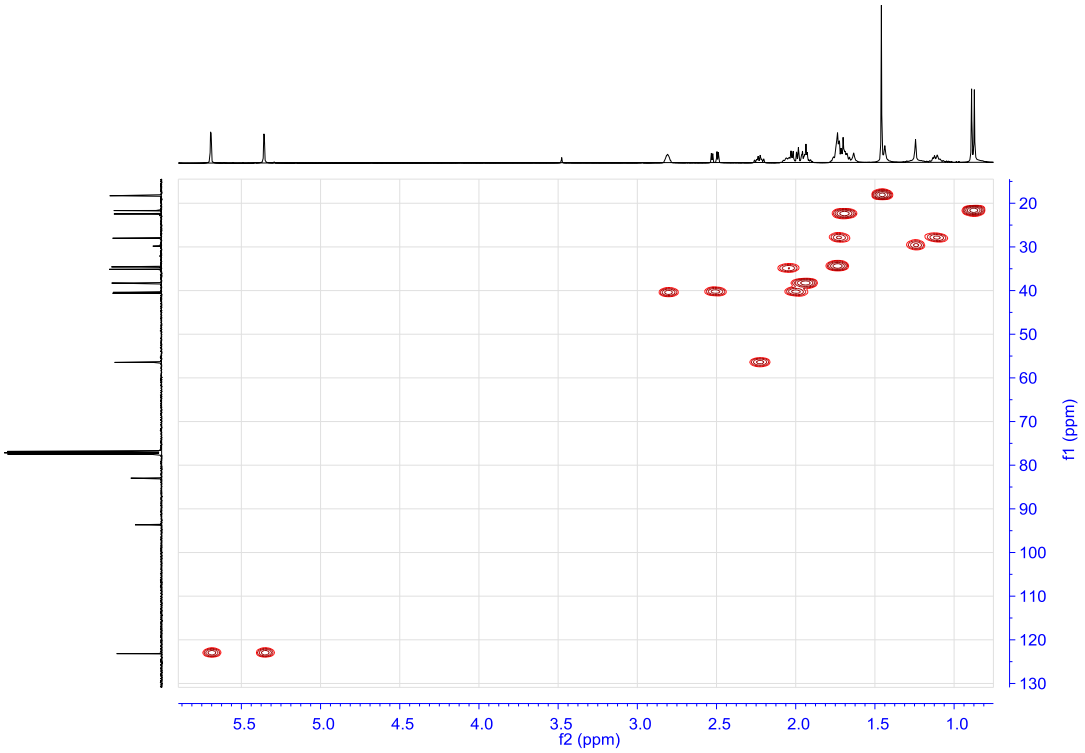

Figure S20 HSQC spectrum of compound **2** (400 MHz, $CDCl_3$)

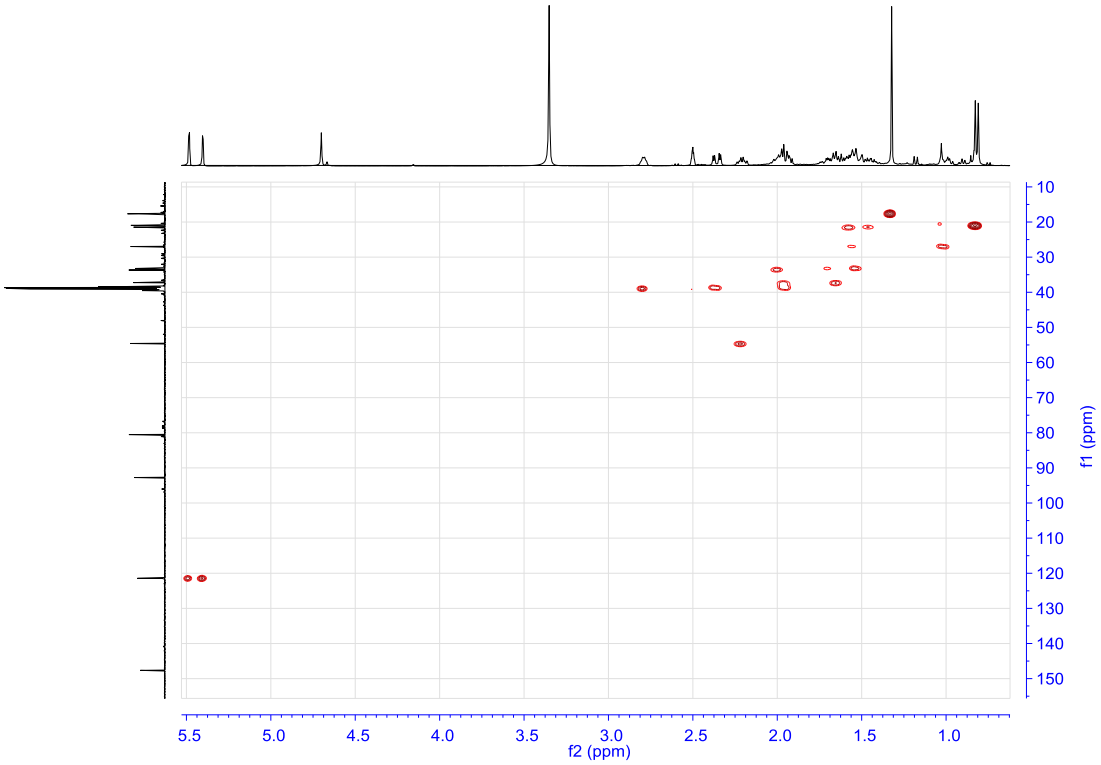

Figure S21 HSQC spectrum of compound **2** (400 MHz, DMSO-d_6)

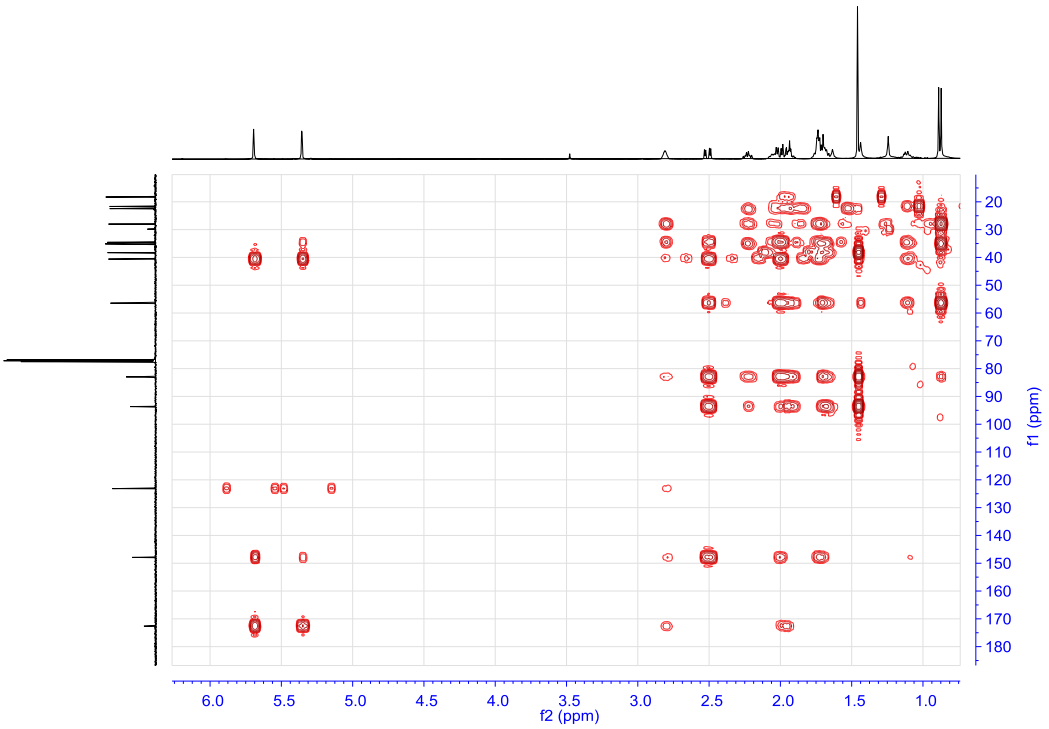

Figure S22 HMBC spectrum of compound **2** (400 MHz, $CDCl_3$)

Figure S23 HMBC spectrum of compound **2** (400 MHz, DMSO-d_6)

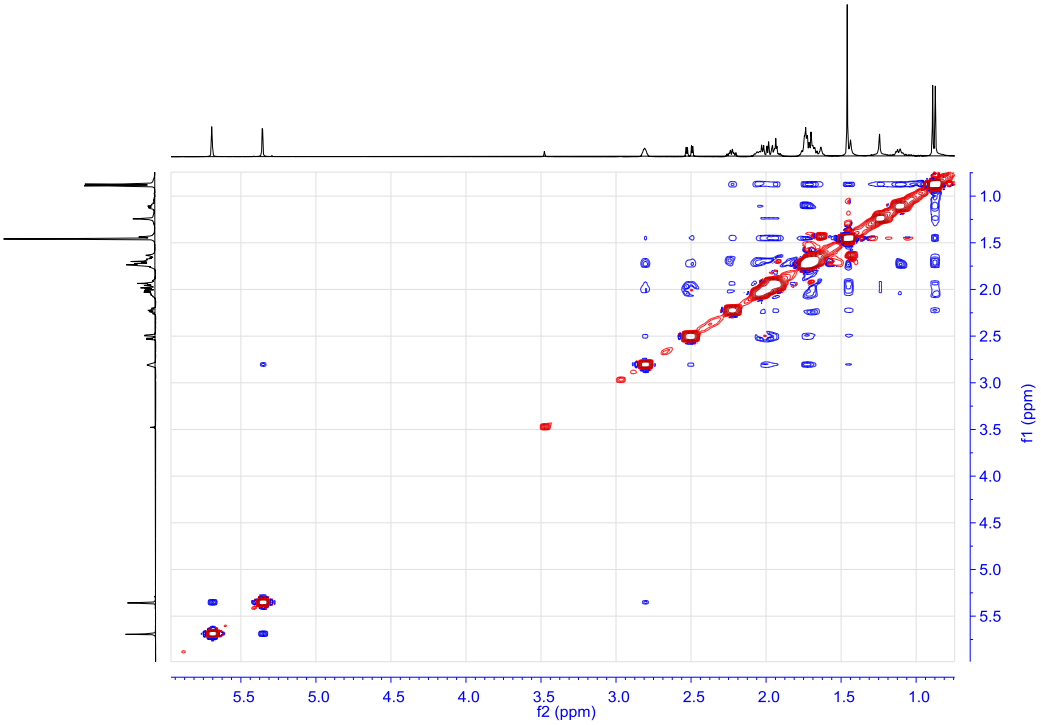

Figure S24 NOESY spectrum of compound **2** (400 MHz, $CDCl_3$)

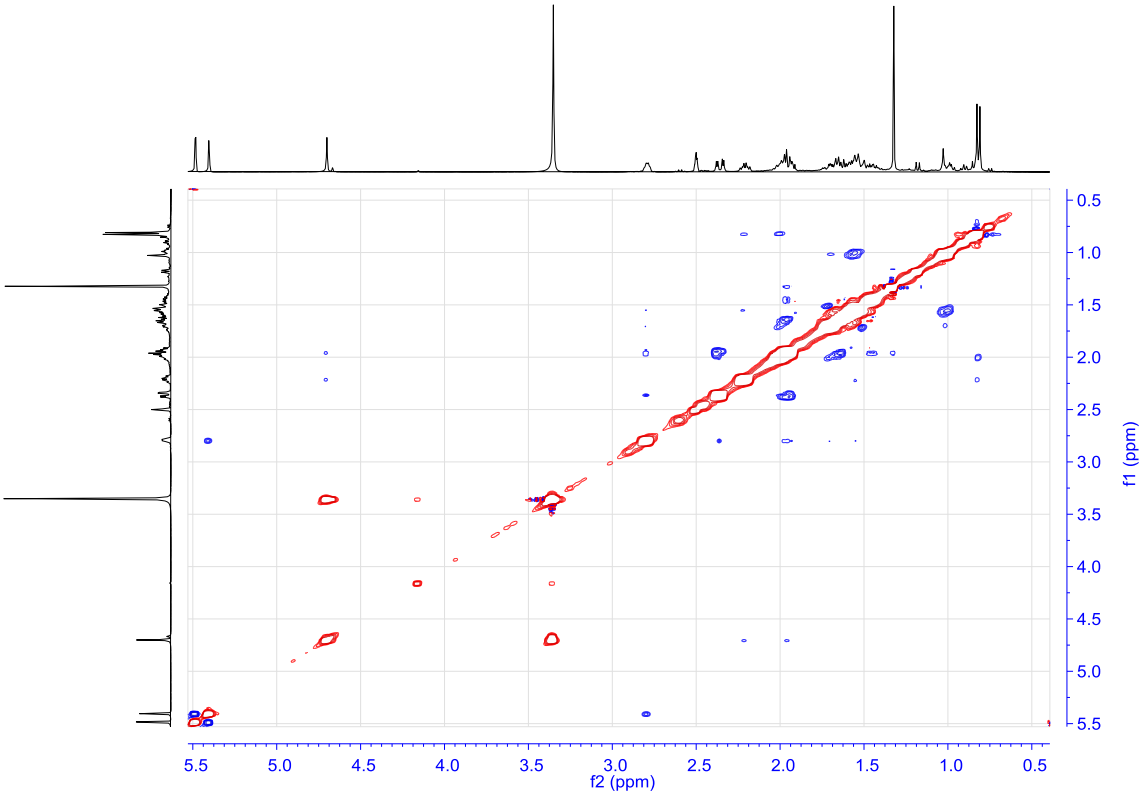

Figure S25 NOESY spectrum of compound **2** (400 MHz, DMSO-d_6)

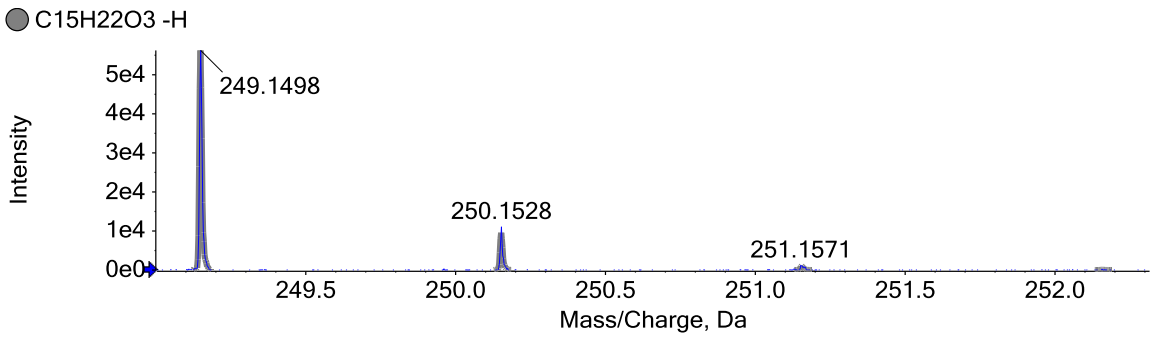

Figure S26 HR-ESI-TOF-MS spectrum of compound **3**

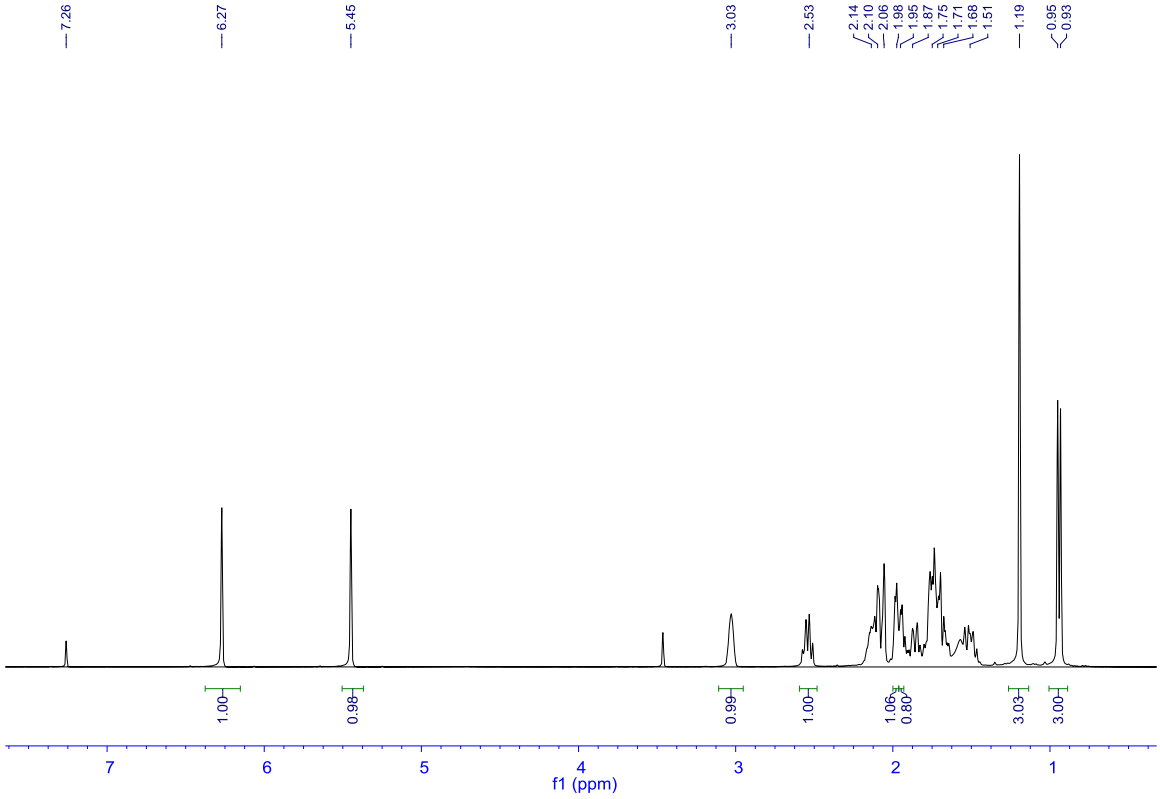

Figure S27 ^{1}H-NMR spectrum of compound **3** (400 MHz, $CDCl_3$)

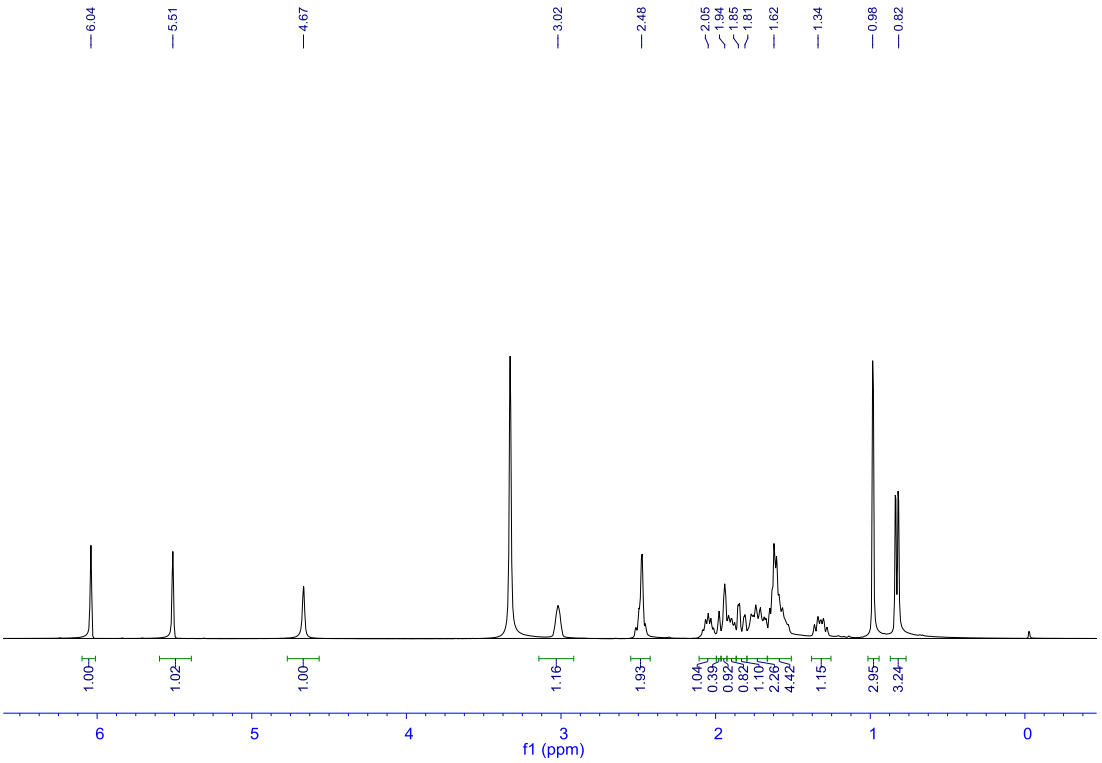

Figure S28 ^{1}H-NMR spectrum of compound **3** (400 MHz, DMSO-d_6)

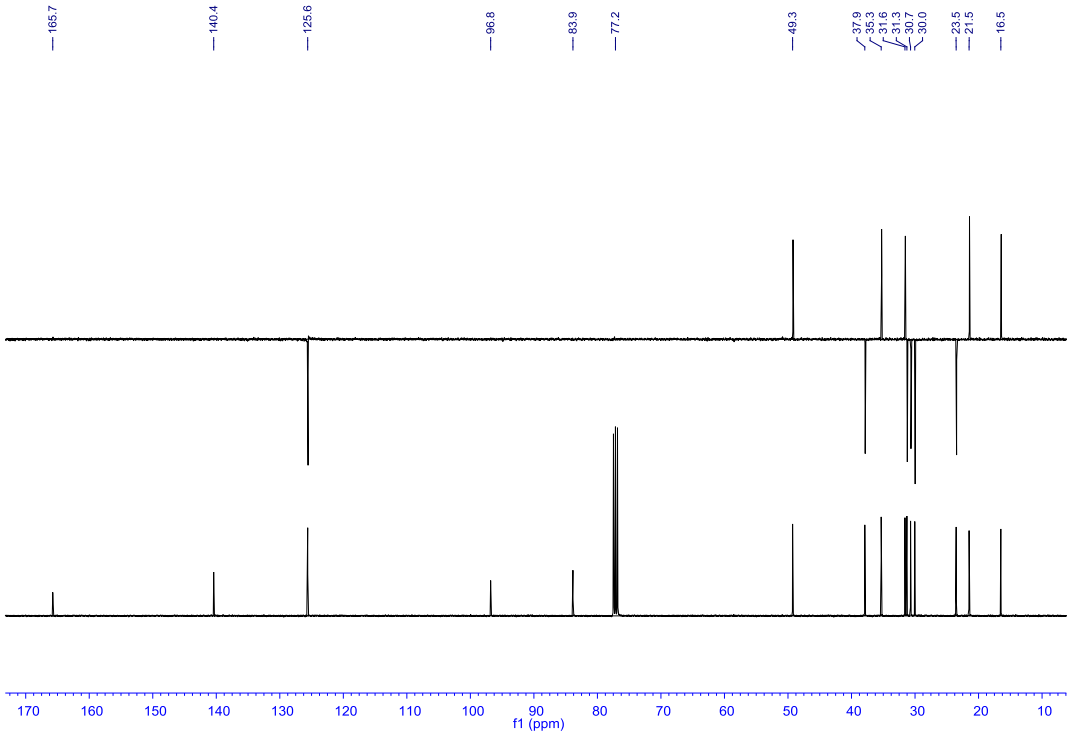

Figure S29 ^{13}C-NMR spectrum of compound **3** (100 MHz, $CDCl_3$)

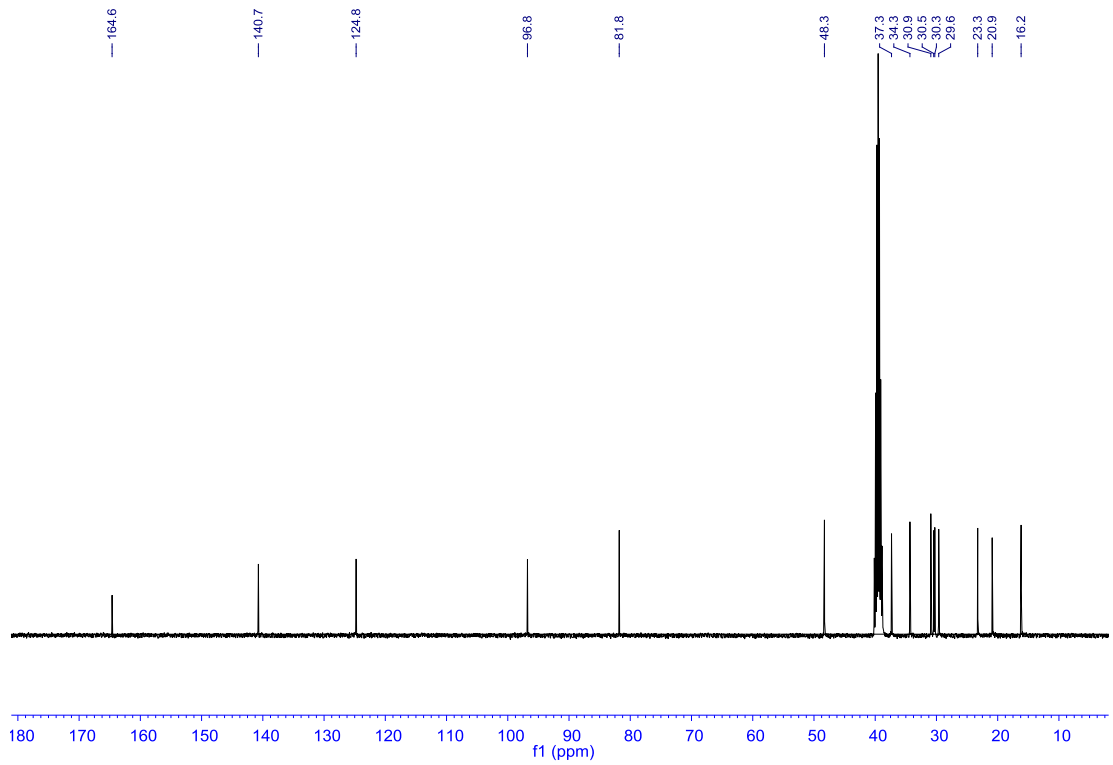

Figure S30 ^{13}C-NMR spectrum of compound **3** (100 MHz, DMSO-d_6)

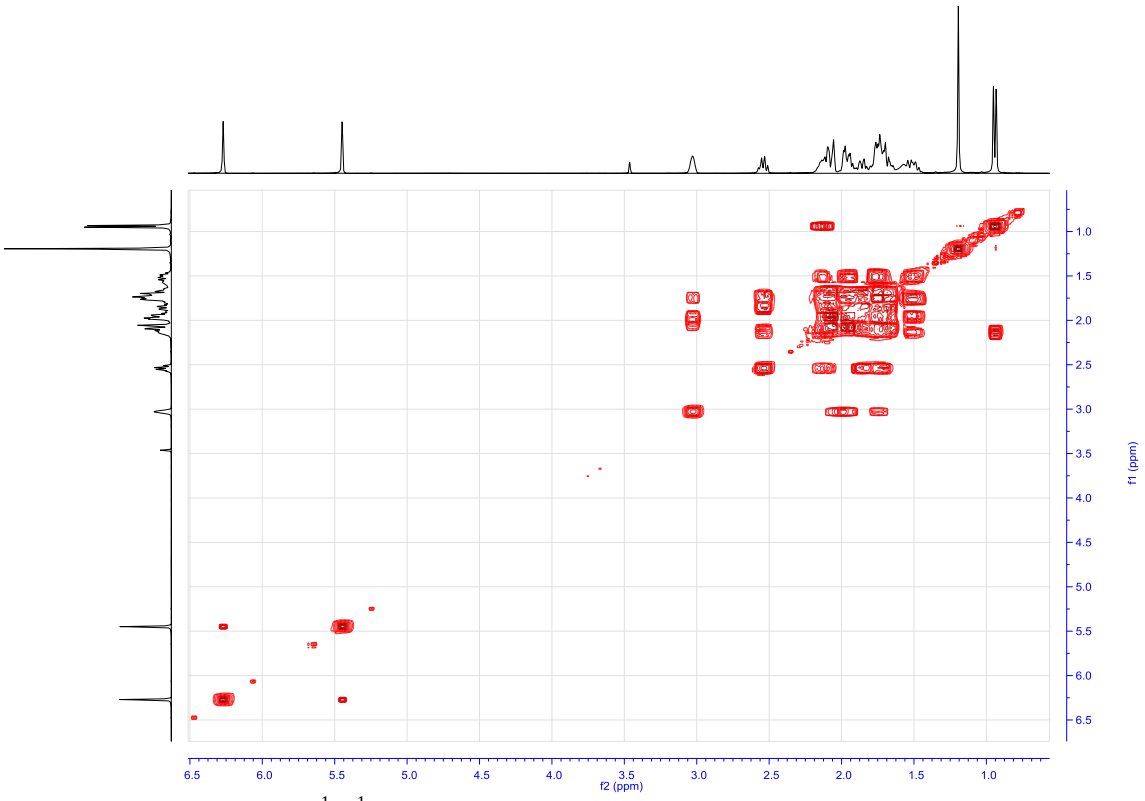

Figure S31 ^{1}H-^{1}H COSY spectrum of compound **3** (400 MHz, $CDCl_3$)

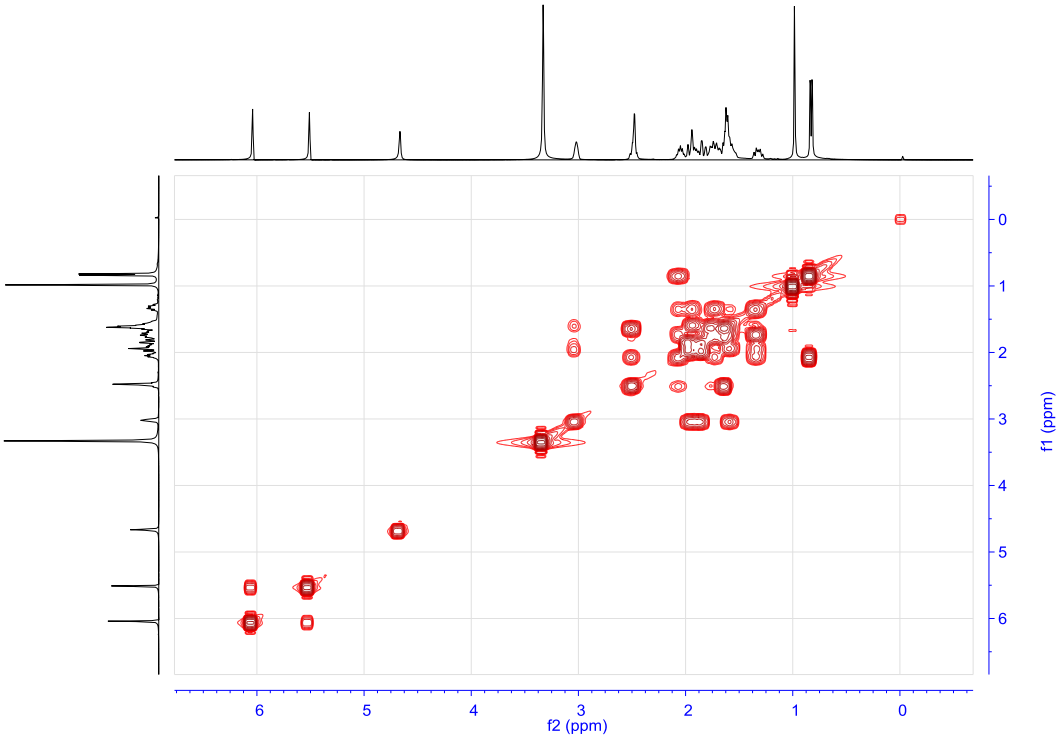

Figure S32 ^{1}H-^{1}H COSY spectrum of compound **3** (400 MHz, DMSO-d_6)

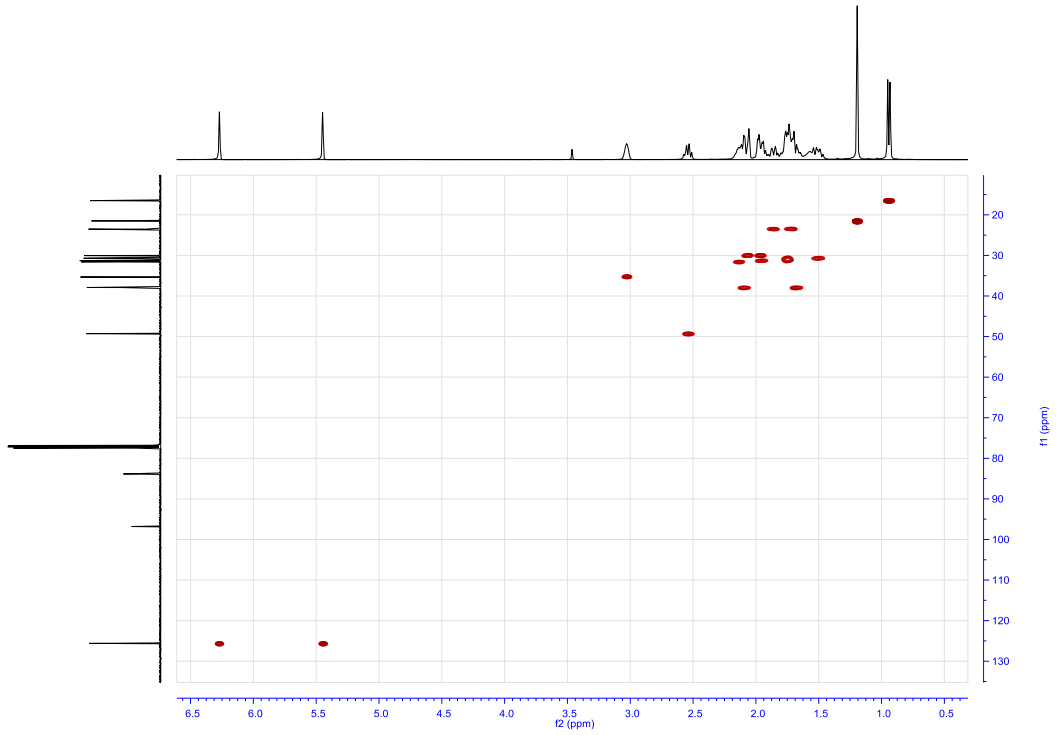

Figure S33 HSQC spectrum of compound **3** (400 MHz, $CDCl_3$)

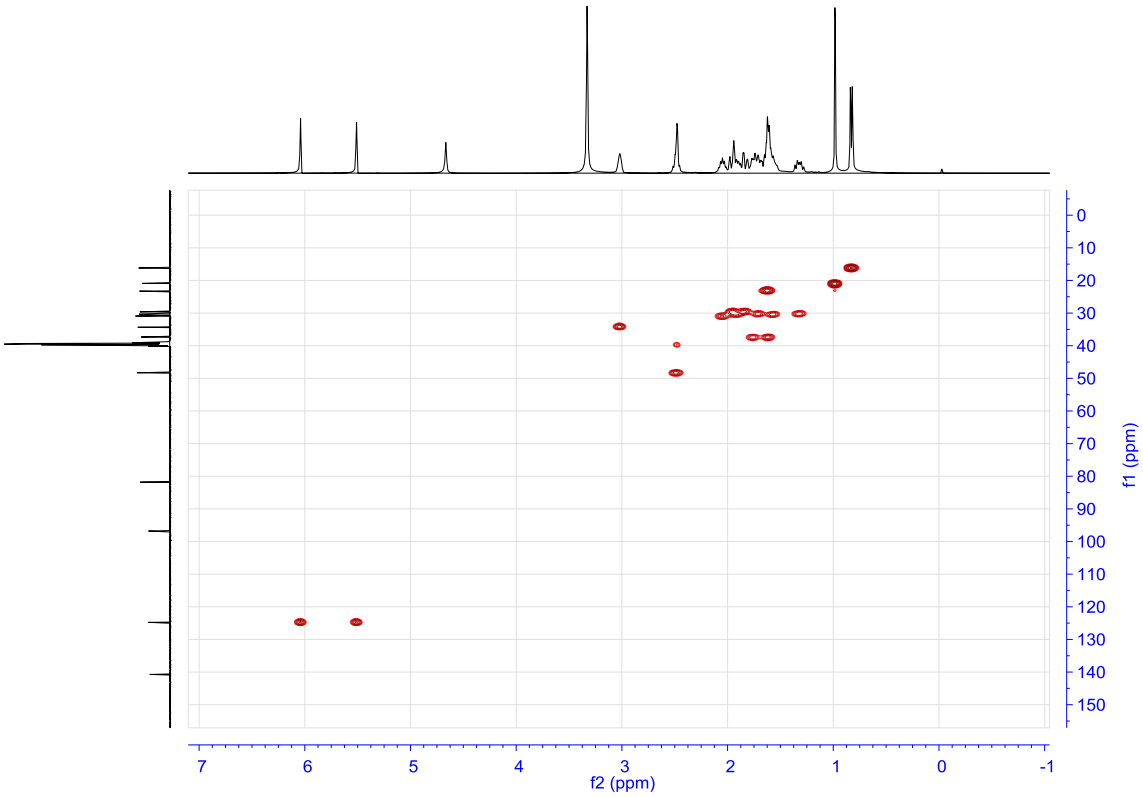

Figure S34 HSQC spectrum of compound **3** (400 MHz, DMSO-d_6)

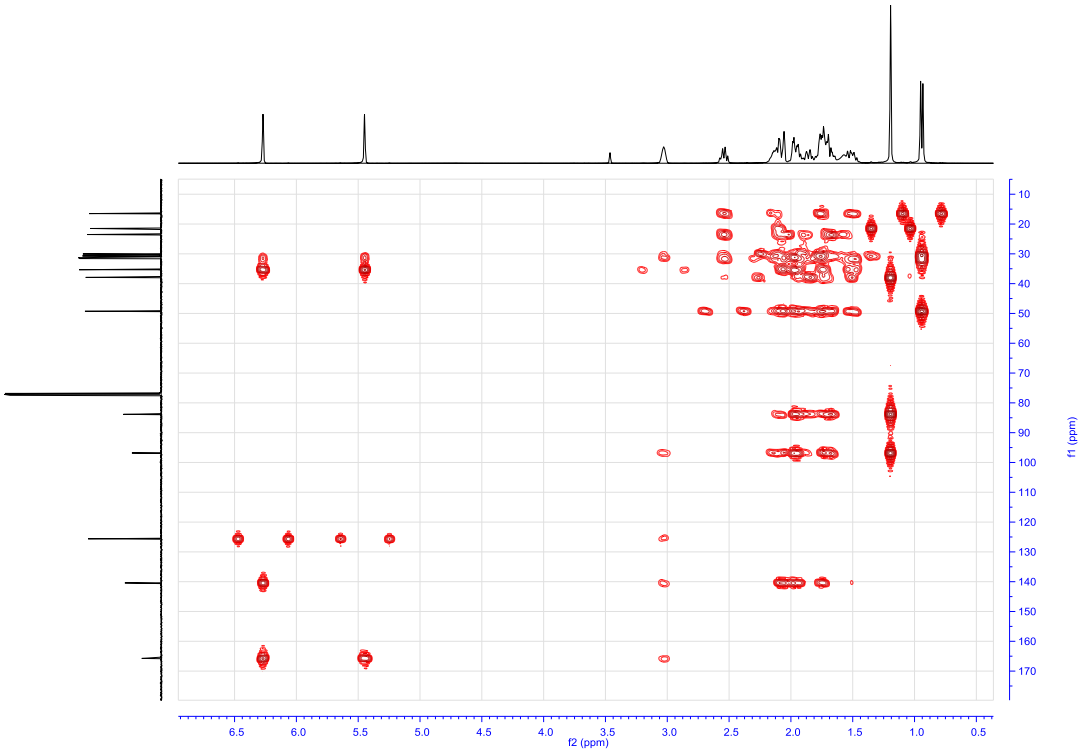

Figure S35 HMBC spectrum of compound **3** (400 MHz, $CDCl_3$)

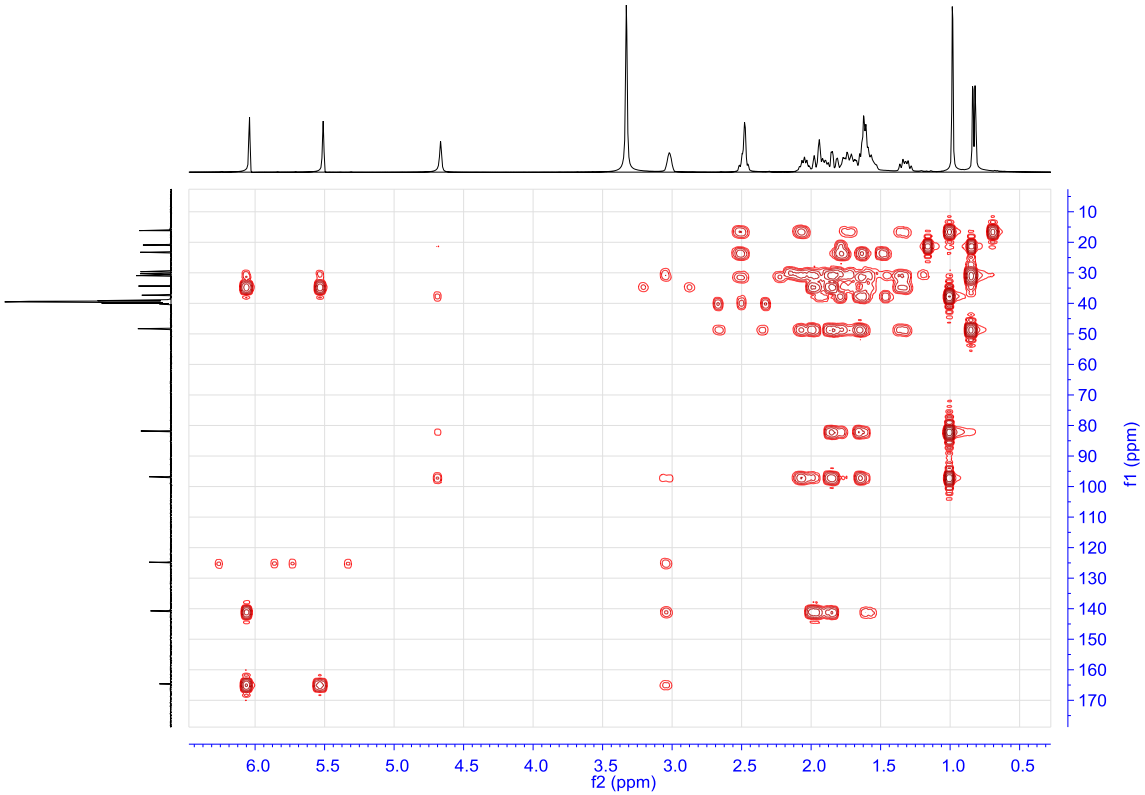

Figure S36 HMBC spectrum of compound **3** (400 MHz, DMSO-d_6)

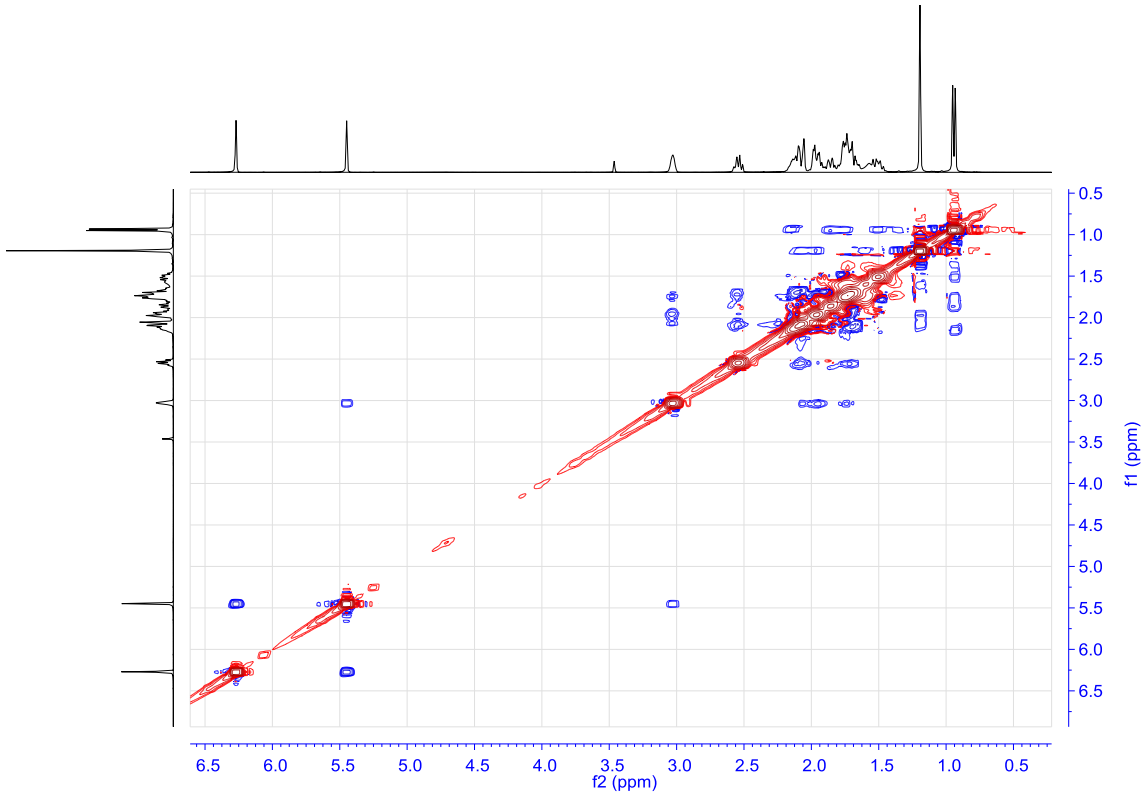

Figure S37 NOESY spectrum of compound **3** (400 MHz, $CDCl_3$)

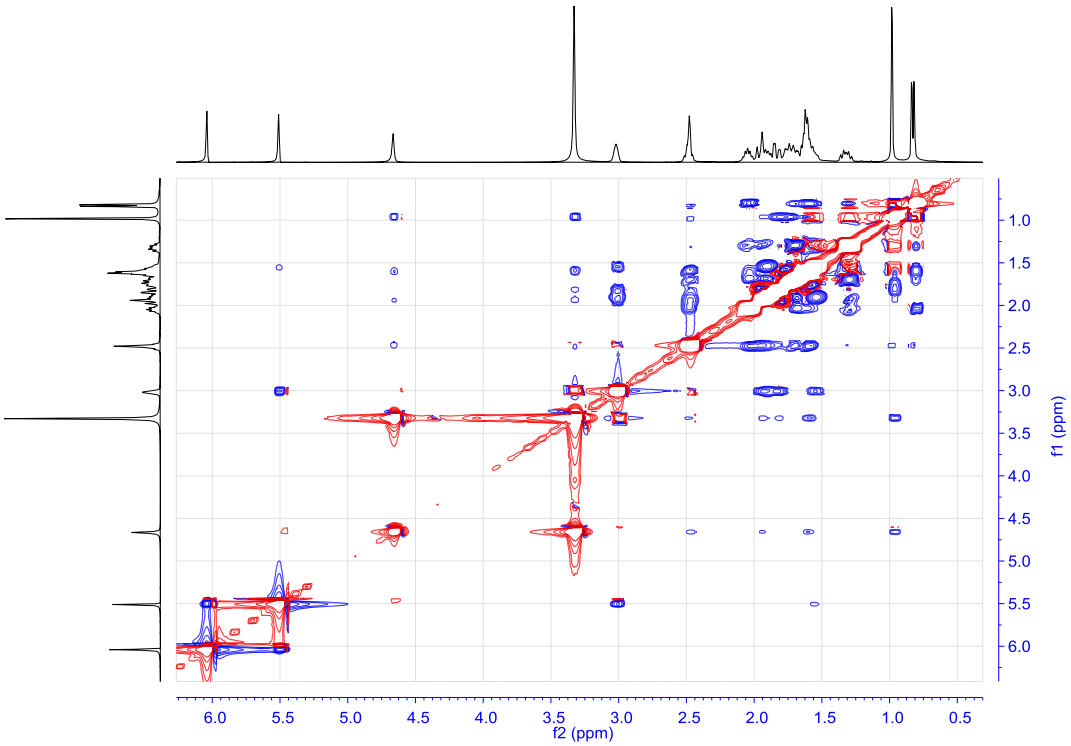

Figure S38 NOESY spectrum of compound **3** (400 MHz, DMSO)